

Chapter 3

The Kongsfjorden Transect: Seasonal and Inter-annual Variability in Hydrography



Vigdis Tverberg, Ragnheid Skogseth, Finlo Cottier, Arild Sundfjord, Waldemar Walczowski, Mark E. Inall, Eva Falck, Olga Pavlova, and Frank Nilsen

Abstract The Kongsfjorden conductivity, temperature and depth (CTD) Transect has been monitored annually since 1994. It covers the full length of the fjord and the shelf, and the upper part of the shelf slope outside Kongsfjorden. In addition to CTD profiles, data from vessel-mounted Acoustic Doppler Current Profiler (ADCP) and moorings have been collected. Previous studies noted that Atlantic Water (AW) from the West Spitsbergen Current was observed in the fjord every summer, but to a varying extent. The prolonged monitoring provided by the Kongsfjorden Transect data set examined here reveals continuous variations in AW content and vertical distribution in the fjord, both on seasonal and inter-annual timescales. Our focus in

V. Tverberg (✉)

Faculty of Biosciences and Aquaculture, Nord University, Bodø, Norway
e-mail: vigdis.tverberg@nord.no

R. Skogseth

The University Centre in Svalbard, Longyearbyen, Norway

F. Cottier

Scottish Association for Marine Science, Scottish Oceans Institute, Oban, UK

Department of Arctic and Marine Biology, Faculty of Biosciences, Fisheries and Economics, UiT The Arctic University of Norway, Tromsø, Norway

A. Sundfjord · O. Pavlova

Norwegian Polar Institute, Fram Centre, Tromsø, Norway

W. Walczowski

Institute of Oceanology, Polish Academy of Science, Sopot, Poland

M. E. Inall

Scottish Association for Marine Science, Oban, Argyll, UK

Department of Geosciences, University of Edinburgh, Edinburgh, UK

E. Falck · F. Nilsen

The University Centre in Svalbard, Longyearbyen, Norway

Geophysical Institute, University of Bergen, Bergen, Norway

© Springer Nature Switzerland AG 2019

H. Hop, C. Wiencke (eds.), *The Ecosystem of Kongsfjorden, Svalbard*,
Advances in Polar Ecology 2, https://doi.org/10.1007/978-3-319-46425-1_3

this paper is on this variable content of AW in Kongsfjorden, the forcing mechanisms that may govern the inflow of this water mass, and its distribution in the fjord. We classify three winter types linked to three characteristic scenarios for winter formation of water masses. During the historically typical winters of type “Winter Deep”, deep convection, often combined with sea ice formation, produces dense winter water that prevents AW from entering Kongsfjorden. Summer inflow of AW starts when density differences between fjord and shelf water allows for it, and occurs at some intermediate depth. During winters of type “Winter Intermediate”, AW advects into the fjord along the bottom via Kongsfjordrenna. Winter convection in Kongsfjorden will then be limited to intermediate depth, usually producing very cold intermediate water. Deep AW inflow continues during the following summer. A winter of type “Winter Open” seems to develop when open water convection produces very dense shelf water, and AW winter advection into Kongsfjorden occurs at the surface. Summer AW inflow is rather shallow after such winters. We find that variations between Winter Deep and Winter Intermediate winters are due to inherent natural variability. However, the Winter Open winters seem to be a consequence of the general trend of atmospheric and oceanic warming, and, more specifically, of the decreasing sea ice cover in the Arctic region. The Winter Open winters have all occurred after an unusual flooding of AW onto the West Spitsbergen shelf in February 2006.

Keywords Kongsfjorden · Atlantic Water · Hydrography · Water masses · Exchange

Abbreviations

ADCP	Acoustic Doppler Current Profiler
ArW	Arctic Water
AW	Atlantic Water
CTD	Conductivity Temperature Depth
ESC	East Spitsbergen Current
GSW	Gibbs Sea Water
IOPAN	Institute of Oceanology, Polish Academy of Sciences
IW	Intermediate Water
LW	Local Water
NPI	Norwegian Polar Institute
PSS78	Practical Salinity Scale 1978
SAMS	Scottish Association for Marine Science
SNR	Signal to Noise Ratio
SPC	Spitsbergen Polar Current
SW	Surface Water
TAW	Transformed Atlantic Water
TEOS-10	Thermodynamic Equation of Sea Water 2010

TS	Temperature-Salinity
UiB	University of Bergen
UNIS HD	UNIS Hydrographic Database
UNIS	The University Centre in Svalbard
WCW	Winter Cooled Water
WSC	West Spitsbergen Current

3.1 Introduction

The Kongsfjorden Transect is a set of CTD and biological stations distributed along a line from the head of Kongsfjorden to the continental slope west of Spitsbergen, and includes station locations that were identified and then commonly occupied after the Kongsfjorden workshop organized in Longyearbyen in 2000. The main outcome of this workshop was two review papers, one on the marine ecosystem (Hop et al. 2002) and one on the physical environment of Kongsfjorden (Svendsen et al. 2002). Subsequently, the number of hydrographic observations along the Kongsfjorden transect has expanded extensively, resulting in many publications. Here we review these publications, and introduce further unpublished data from the collection of observations. Summer observations of hydrography along the Kongsfjorden transect started in 1994 and continued every summer from 1997 to 2014. Winter observations from 13 of these years are also available, as well as time series from moorings inside Kongsfjorden. This expanded data set allows for deeper insight into the seasonal and inter-annual variations in oceanographic conditions in Kongsfjorden and also captures the interaction with the shelf and slope water masses.

In this review, we focus on the interaction between the fjord/shelf and the Atlantic Water (AW) from the West Spitsbergen Current (WSC). The WSC is topographically steered along the continental slope (Walczowski and Piechura 2007), and is a major source of warm and saline AW to the Arctic Ocean (Polyakov et al. 2005). The WSC is subject to cooling and freshening as it flows northward (Saloranta and Haugan 2004), and interactions with West Spitsbergen fjords such as Kongsfjorden can make a significant contribution to this modification. Understanding the mechanisms governing the interaction between the WSC and West Spitsbergen fjords (here represented by Kongsfjorden) is therefore important, not only for explaining environmental conditions inside the fjords, but also for explaining variability in the Arctic Ocean. Svendsen et al. (2002) and subsequent publications (Cottier et al. 2005; Nilsen et al. 2008) were able to observe that the volume and resulting influence from AW could change substantially from one summer to the next. This year-to-year variability in AW content in Kongsfjorden has been referred to as ‘warm’ and ‘cold’ years (Cottier et al. 2005) in line with earlier biological studies of West Spitsbergen fjords (Weslawski and Adamski 1987) as well as on a more regional scale (Furevik 2001). This review places these observations in a seasonal and inter-annual perspective. The West Spitsbergen fjords are separated from the WSC by a shallow shelf, along which there is a northward flowing coastal current advecting

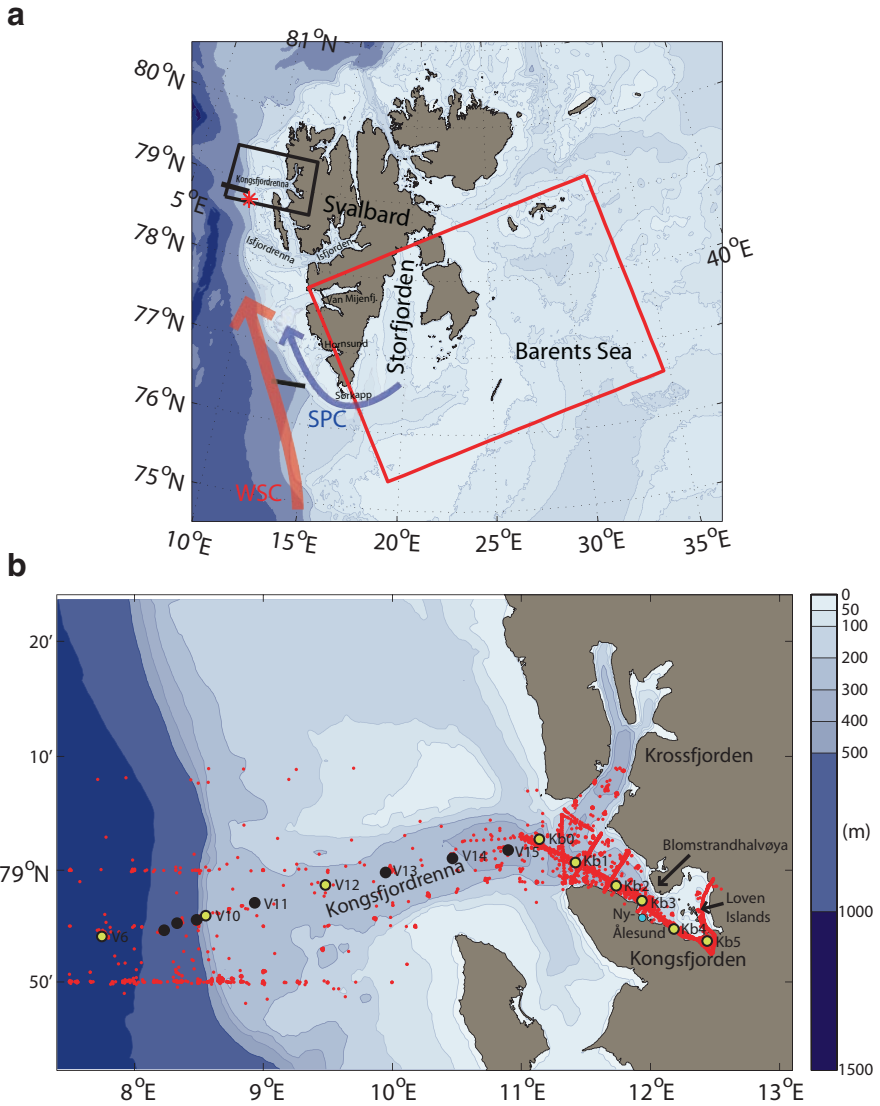


Fig. 3.1 (a) Map of Svalbard area. ERA Interim surface heat flux data extracted from red star position, and National Snow and Ice Data Center (NSIDC) monthly sea-ice data from within red box. Black transect lines show locations of CTD data used to produce data in Fig. 3.4. WSC West Spitsbergen Current, SPC Spitsbergen Polar Current (coastal current). Map inside black box shown in (b) Map of Kongsfjorden with adjacent shelf area. Red dots are all CTD positions included in this review. Black circles are positions of the CTD stations comprising the Kongsfjorden transect, also listed in Table 3.1. The black circles with yellow center are also biological stations. Ny-Ålesund is indicated with cyan dot

Arctic Water (ArW) and drift ice from Storfjorden and the Barents Sea (Fig. 3.1). This current was termed the Spitsbergen Polar Current (SPC) by Helland-Hansen and Nansen (1909), but is now sometimes termed the Sørkapp Current, or the continuation of the East Spitsbergen Current (ESC). Troughs cross the shelf from the shelf edge towards each fjord. In this paper we focus on the trough outside Kongsfjorden, called Kongsfjordrenna (Fig. 3.1). A substantial part of the AW inflow to the fjords is topographically steered along these troughs as modelled by Nilsen et al. (2016), where they named this flow the Spitsbergen Trough Current. Throughout this paper we use the term ‘Kongsfjordrenna’ when we specifically discuss the topographically-steered AW inflow to Kongsfjorden, while in most cases we use the term ‘shelf’ when we mean the area between the WSC and Kongsfjorden.

Mooring temperature data from within Kongsfjorden have revealed that unusually large volumes of AW entered the fjord during February 2006 (Cottier et al. 2007), increasing the annual mean temperature in Kongsfjorden by 2 °C in 2006. Substantial sea ice melting was also observed around Svalbard that winter, following a tendency of increased winter sea ice melting in the region (Onarheim et al. 2014). One particular question that the present review intends to answer is: Was the February 2006 AW event a tipping point for the environmental conditions and biological response in Kongsfjorden, or was it part of the natural variability? The 2 °C increase in yearly mean temperature in Kongsfjorden has not been permanent, and the degree of ice melting in the region has been observed to vary inter-annually. We use two decades of CTD observations along the Kongsfjorden Transect as well as a decade of mooring data from Kongsfjorden, a large portion of which have not been published previously, to shed light on the reasons for the observed inter-annual variations. The paper is organized with an overview of the data first, followed by an extensive presentation of the forcing mechanisms that determine water mass transformations in the Kongsfjorden Transect. We then proceed by showing how variability in the forcing mechanisms affects the seasonal cycle and is consequently leading to inter-annual variability in hydrography as well as AW content in Kongsfjorden. Detailed descriptions of yearly winter and summer versions of the Kongsfjorden Transect hydrography are given in Appendix A, while in the discussion we relate our findings to inter-annual variations in other environmental factors, especially the Arctic ice cover.

3.2 Observations

The Geophysical Institute at the University of Bergen (UiB) in Norway initiated monitoring of the physical oceanography of Kongsfjorden and the adjacent shelf during a September cruise in 1994. This initiative was soon supported by two additional Norwegian institutions, The University Centre in Svalbard (UNIS) and the Norwegian Polar Institute (NPI), with a joint cruise in December 1994. In 1996, Institute of Oceanology Polish Academy of Sciences (IOPAN) in Sopot, Poland, started their monitoring program with yearly summer cruises to the west coast of Spitsbergen and

Table 3.1 Station list of the section referred to as the Kongsfjorden Transect. Stations named with italic letters are CTD stations only, the other stations are also biological stations. The station locations are indicated in Fig. 3.1b

Location	Latitude	Longitude	Bottom depth (m)
Kb5	N78 53.70	E012 26.44	85
Kb4	N78 54.75	E012 11.00	110
Kb3	N78 57.30	E011 56.16	345
Kb2	N78 58.63	E011 44.19	300
Kb1	N79 00.70	E011 25.24	360
Kb0	N79 02.76	E011 8.50	325
<i>V15</i>	N79 01.78	E010 53.83	320
<i>V14</i>	N79 01.05	E010 27.99	290
<i>V13</i>	N78 59.79	E009 56.99	260
<i>V12</i>	N78 58.70	E009 28.95	225
<i>V11</i>	N78 57.10	E008 56.11	220
<i>V10</i>	N78 55.95	E008 33.28	280
<i>V9</i>	N78 55.58	E008 29.00	500
<i>V8</i>	N78 55.28	E008 20.00	750
<i>V7</i>	N78 54.65	E008 14.01	870
<i>V6</i>	N78 54.11	E007 44.99	1140

Kongsfjorden, undertaking both physical and biological sampling. In 2000, biologists at the Norwegian Polar Institute started biological sampling at stations initiated by IOPAN (Kb0–Kb5), and with additional CTD (*V6–V15*) and biological stations (*V6*, 10 and 12) on the adjacent shelf and slope. These sampling stations evolved into what is now called ‘the Kongsfjorden Transect’. The station positions in the Kongsfjorden Transect are listed in Table 3.1, and indicated in Fig. 3.1b.

The assemblages of CTD surveys that provide data for this review paper, are extracted from the UNIS Hydrographic Database (UNIS HD), a CTD database for the whole Svalbard region. Our subset of this database contains stations sampled during the period August 1906 – May 2015 (red dots in Fig. 3.1b), and it includes all data sampled over the period 1994–2014, as described in the previous paragraph. We here name our subset the Kongsfjorden Transect data. The Norwegian Polar Institute has provided a few additional data from July 2015 and July 2016. The CTD stations in the database do not all follow the defined positions of the Kongsfjorden Transect (see Fig. 3.1b). However, since biological data are associated with these stations, when we show section plots, we have chosen to interpolate all data onto a line approximately following the CTD transect listed in Table 3.1. Moreover, the transect stations follow Kongsfjorden and Kongsfjordrenna more or less along the central axis, while the expected path of geostrophic AW advection will be along the southern side of Kongsfjordrenna. At Kb3 the transect is close to the expected topographically steered AW advection inside Kongsfjorden, as the current tends to follow the 200 m isobath. Data coverage is best for summer months (July–September). However, there were quite a few surveys in the period January to May as well,

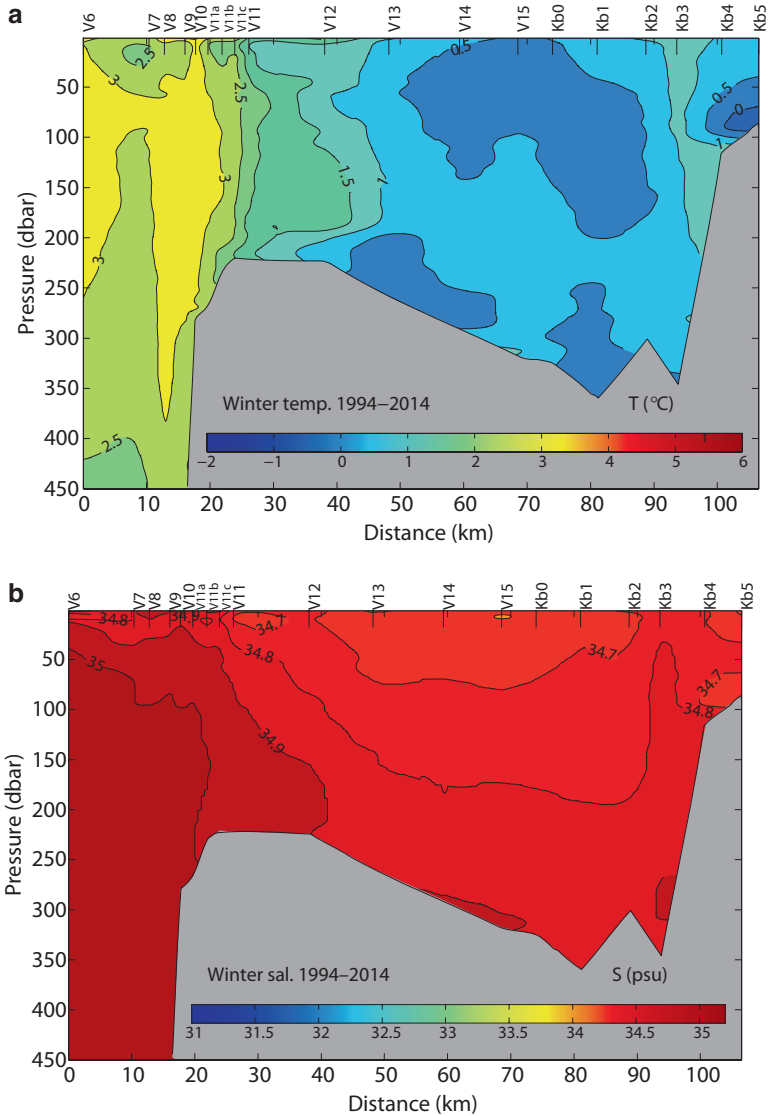


Fig. 3.2 Mean winter temperature and salinity along the Kongsfjorden transect, based on all available Kongsfjorden Transect data between 1994 and 2014. The entrance of the Kongsfjorden-Krossfjorden system is located between stations Kb0 and Kb1

making it possible to present winter (January–May) and summer (July–September) versions of the transect. The interpolation procedure is as follows. The data from the CTD stations are averaged into bins between the positions comprising the Kongsfjorden Transect (Table 3.1), then the non-uniform binaveraged temperature, salinity and density transects are interpolated onto a regular grid with 500 m hori-

zonal resolution using the kriging interpolation method. The method interpolates between data points, and extrapolates beyond data points, similar to objective mapping (Emery and Thomson 2014). Regions with horizontal isolines in temperature, salinity and density can be indicative of bad data coverage. The two panels in Fig. 3.2 show mean winter (January–May) distribution of temperature and salinity in the Kongsfjorden Transect, based on all winter data collected during the bi-decadal period 1994–2014 (data from 13 of the possible 21 winters). The mean summer (July–September) distribution of temperature and salinity in the Kongsfjorden Transect during the two decades 1994–2014 (data from 19 of the possible 21 summers) are shown in the two panels in Fig. 3.3. The entrance of the Kongsfjorden-Krossfjorden system is located between stations Kb0 and Kb1, and the shelf edge at V10, separating the transect into three regions: the fjord, the SPC region on the shelf (Kongsfjordrenna) and the WSC over the continental slope. Throughout the paper, we use the old standard for salinity; Practical Salinity PSS78 as opposed to the new standard Absolute Salinity in TEOS-10 (Millero et al. 2008), mainly to avoid confusion in water mass characteristics.

Mooring data have been available from various locations in the central Kongsfjorden basin since April 2002, and nearly continuously since September 2003. The moorings have been well equipped with temperature sensors, an upward looking ADCP (often with both upward and downward looking instruments, since 2012), and two or three conductivity loggers. Over time, additional parameters have been added, including fluorescence and PAR loggers and 21-bottle sediment traps. These moorings were designed by Scottish Association for Marine Science (SAMS), and deployed in Kongsfjorden in a joint effort with different Norwegian institutions (NPI, UiB and UNIS). We refer to them as SAMS moorings in an overview of all moorings deployed in Kongsfjorden (Table 3.2). Time series of temperature and fluorescence from the SAMS moorings are presented in Hegseth et al. (Chap. 6), and we will refer to those Figs. later in the review. UNIS and UiB have had additional, more conventional moorings equipped with current meters with temperature, conductivity and pressure sensors at up to three depths. From September 2002 to September 2003 and from August 2004 to September 2005, this type of mooring was deployed on the southern side of the entrance of Kongsfjorden in the central basin (U1 in Table 3.2). Then it was redeployed each year from September 2005 to August 2015 further inwards in the fjord, close to Blomstrandhalvøya (H1 in Table 3.2; Fig. 3.1b). Table 3.2 contains observation periods and positions of moorings in Kongsfjorden. It is not a complete list, only the ones from which data have been used here for tidal analysis, and presented in Hegseth et al. (Chap. 6). A more complete presentation of SAMS mooring data can be found in Wallace et al. (2010).

3.3 Forcing Mechanisms

The seminal review by Svendsen et al. (2002) distinguished between internal and external forcing mechanisms contributing to water mass transformations in Kongsfjorden. The internal mechanisms act within the fjord, and comprise

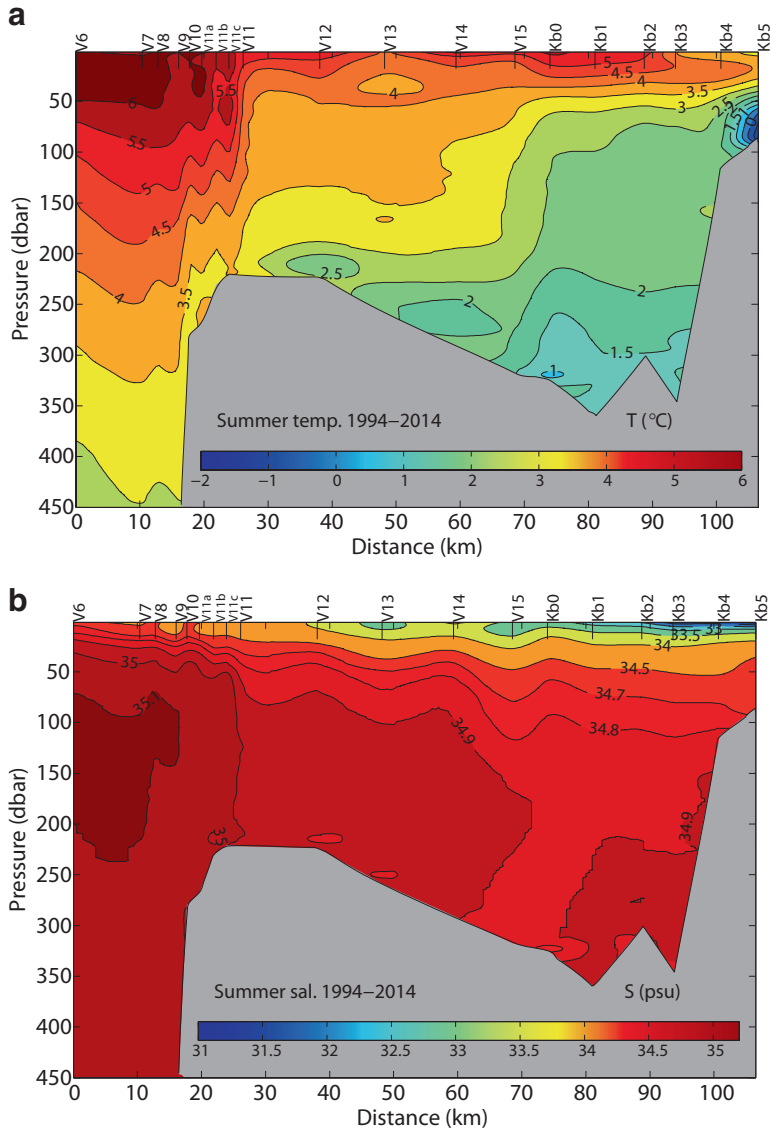


Fig. 3.3 Mean summer temperature and salinity along the Kongsfjorden transect, based on all available Kongsfjorden Transect data between 1994 and 2014. The entrance of the Kongsfjorden-Krossfjorden system is located between stations Kb0 and Kb1

freshwater runoff, solar heating, wind forcing, vertical mixing and sea ice formation, and modifications on internal circulation from the effects of the rotation of the earth. Svendsen et al. (2002) emphasized the upper layer circulation caused by freshwater runoff and wind forcing, and on rotational effects on the deep circulation. These physical processes were further reviewed by Cottier et al. (2010).

Table 3.2 Mooring positions in Kongsfjorden, including selected periods where tidal analysis were made for this review

Mooring	Date from	Date to	Latitude	Longitude	Bottom (m)	
D1	16 April 2002	23 June 2002	N79 03.25	E011 18.00	212	SAMS
	16 April 2002	23 June 2002				Tidal anal.
D2	3 July 2002	28 Sep 2002	N79 03.336	E011 17.24	213	SAMS
	3 July 2002	28 Sep 2002				Tidal anal.
D3	24 May 2003	6 Sep 2003	N78 58.307	E011 39.114	260	SAMS
	24 May 2003	6 Sep 2003				Tidal anal.
D4	9 Sep 2003	22 Aug 2004	N78 58.32	E011 38.75	270	SAMS
	9 Sep 2003	16 Oct 2003				Tidal anal.
D5	23 Aug 2004	14 Sep 2005	N78 57.443	E011 49.365	170	SAMS
D5-1	23 Aug 2004	10 Oct 2004	N78 57.443	E011 49.365	170	Tidal anal.
D5-2	11 Oct 2004	14 Sep 2005	N78 57.443	E011 49.365	170	Tidal anal.
D6	16 Sep 2005	30 May 2006	N79 01.21	E011 46.45	210	SAMS
D7	06 June 2006	25 August 2007	N79 01.20	E011 46.417	209	SAMS
D8	30 Aug 2007	19 Aug 2008	N78 57.44	E011 49.60	178	SAMS
D9	04 Sept 2008	22 Aug 2009	N78 59.18	E011 20.929	209	SAMS
D10	06 Sept 2009	16 Sept 2010	N78 57.75	E011 45.556	225	SAMS
D11	26 Sept 2010	02 Sept 2011	N78 57.75	E011 45.556	221	SAMS
D12	26 Sept 2011	08 Sept 2012	N78 57.75	E011 45.556	251	SAMS
D13	03 Oct 2012	03 Sept 2013	N78 57.73	E011 48.428	241	SAMS
D14	05 Oct 2013	09 Sept 2014	N78 57.75	E011 48.30	230	SAMS
U1	Sep 2002	Sep 2003	N78 58.681	E011 32.490	202	UNIS
U1-1	24 May 2003	6 Sep 2003				Tidal anal.
U1	Sep 2004	Sep 2005	N78 58.681	E011 32.490	202	UNIS
U1-2	11 Oct 2004	24 Jan 2005				Tidal anal.
H1	Sep 2005	Aug 2015	N78 58.382	E011 58.613	218	UNIS
	27 Mar 2015	26 Aug 2015				Tidal anal.

External mechanisms are acting outside of the fjord itself, and they are important in determining the volume and timing of AW present on the shelf (Cottier et al. 2005). Svendsen et al. (2002) briefly touched on this issue, suggesting wind-driven upwelling and downwelling associated with offshore and onshore Ekman transport combined with ageostrophic processes at the shelf-edge front between AW in the WSC and the shelf water as the governing mechanisms. Since then, different mechanisms that can lead to exchange of AW across this shelf-edge front have been suggested (Nilsen et al. 2006; Cottier et al. 2007; Tverberg and Nøst 2009; Teigen et al. 2010, 2011; Tverberg et al. 2014; Inall et al. 2015; Nilsen et al. 2016), involving both ageostrophic and geostrophic processes. These studies illustrate the variety of aspects connected to the exchange mechanisms, which in combination determine how the AW inflow to Kongsfjorden behaves. In this section we first present the WSC and the SPC, then discuss the different aspects of the exchange across the front between these two currents, and the resulting advection of AW towards Kongsfjorden, and why the AW does not always enter Kongsfjorden. Some updates on internal mechanisms are given at the end of the section.

3.3.1 West Spitsbergen Current

Two branches of AW (western and eastern) converge in the region of western Spitsbergen. The western, offshore branch flows along the deep underwater ridges, the eastern branch (core of the WSC) flows along the Barents Sea shelf-break and slope and continues along the western Spitsbergen coast (Walczowski and Piechura 2007). Properties of the eastern, alongshore branch are analyzed more closely here, as it is water from this branch that may flow into the western Svalbard fjords. This current is topographically steered, and the center of the flow is generally situated over the 800 m isobath. Properties of AW vary between successive summers according to the upstream conditions. Moreover, continuing along the Spitsbergen coast, AW in the WSC core becomes colder and fresher due to mixing with ambient waters and exchange with the atmosphere (Boyd and D'Asaro 1994; Saloranta and Haugan 2004). To determine the AW lower limits of temperature and salinity, the AW characteristics ($S > 34.90$, $T > 3$ °C) from Svendsen et al. (2002) were used herein.

We present variability of AW calculated on the basis of the IOPAN summer data for two regions of the WSC (Fig. 3.4). The longest time series in the IOPAN database is for the section along $N76^{\circ}30'$. This section is representative of the general

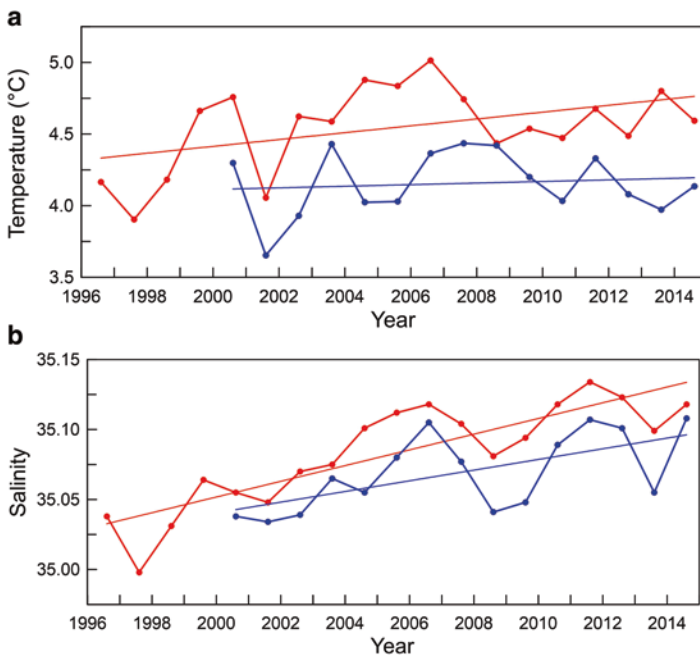


Fig. 3.4 Time series of (a) temperature and (b) salinity of Atlantic Water (AW) ($T > 3$ °C, $S > 34.9$) in the core of the West Spitsbergen Current at latitude $N76^{\circ}30'$, between longitudes $E012^{\circ}30'$ and $E014^{\circ}30'$ (red lines) and at latitude $N78^{\circ}50'$, between longitudes $E007^{\circ}$ and $E009^{\circ}$ (blue lines). Locations of transects are shown in Fig. 3.1a

variability of AW in the WSC (Walczowski 2014). A positive trend of AW temperature and salinity in summer during the period 1996–2014 is evident (Fig. 3.4). The temperature maximum at N76°30' occurs in 2006. Salinity has a more continuous trend, however, with maxima in 2006 and 2011. At the section along N78°50' (close to Kongsfjorden) the salinity variability is very similar to that from N76°30', with values about 0.03 lower. The pattern of temperature variability is somewhat different compared to N76°30', but values are generally lower than at the southern section. AW shows high temperatures in the vicinity of Kongsfjorden in 2003 and during the 2006–2008 period. The summers 2001, 2004, 2005, 2010 and 2013 were relatively cold at the 78°50'N section.

3.3.2 *Spitsbergen Polar Current*

In their review, Svendsen et al. (2002) stated that the West Spitsbergen shelf is occupied by a cold and relatively fresh Arctic type coastal water originating from Storfjorden and the Barents Sea, and carried northwards by a coastal current. As mentioned in the introduction, we adapt the name Spitsbergen Polar Current (SPC) for this coastal current, from Helland-Hansen and Nansen (1909). The water mass transported by the SPC is often called Arctic Water (ArW) with somewhat varying characteristics. In this review, we adapt the characteristics ($-1.5\text{ }^{\circ}\text{C} < T < 1.0\text{ }^{\circ}\text{C}$ and $34.30 < S < 34.80$) suggested by Cottier et al. (2005), which have a salinity range similar to that by Loeng (1991), but with a wider temperature range than suggested by both Loeng (1991) and Helland-Hansen and Nansen (1909). The mean winter characteristics of shelf water (Fig. 3.2) fits into the upper range of our adapted ArW definition. However, our inter-annual comparison of the Kongsfjorden Transect will reveal that the characteristics of the water mass transported by the SPC are even more variable than previously anticipated and do not always fit into the ArW classification.

The general assumption has been that ArW is a version of the Arctic halocline layer, formed by sea ice formation during winter (Rudels et al. 1996). However, some studies (Steele et al. 1995; Cokelet et al. 2008; Tverberg et al. 2014) indicate that drift ice melting in warm water, combined with strong heat loss to the atmosphere, can form a halocline layer similar to that formed by brine release, except that it is possible for the temperature of the layer to be higher than the freezing point. The SPC normally carries drift ice northwards, and ice charts show that this drift ice gradually disappears as it flows northwards, so Tverberg et al. (2014) suggested that interaction with AW in the WSC supplies heat for the melting, indicating that melting can occur even during the winter season, and ensures that the shelf water stays fresh and cold. The combination of ice melting and heat loss to the atmosphere will produce denser melt water than ice melting alone does, implying that a winter melt layer will be thicker than a summer melt layer. Cokelet et al. (2008) even suggested that such a combination; AW losing heat to the atmosphere (90%) and ice melting (10%) forms the Arctic Intermediate Water, found down to

1000 m in the Greenland Sea. When drift ice is not present in the SPC, or north of where it has melted, continuous AW exchange will make the shelf water gradually warmer and more saline, as also Helland-Hansen and Nansen (1909) suggested. This can explain why the northern part of the west Spitsbergen shelf is more of an Atlantic type and less of an Arctic type than further south on the shelf, and that it can be a contribution to the large variability in water mass properties in the SPC. The structure and variability of water mass properties in the SPC have, to our knowledge, never been studied in detail. However, it can be an important factor in the dynamics of the fjord-shelf exchange and interaction with the AW advection towards Kongsfjorden.

3.3.3 Shelf-Edge Front

A classic upwelling mechanism was likely important during the event in February 2006 (Cottier et al. 2007) where it led to deep inflow of AW towards Kongsfjorden. Conservation of volume can be used as a simplified explanation for such a relationship; winds from the north will move water away from the coast in the surface Ekman layer, and this water has to be replaced by ocean water from a deeper level. Northerly winds occurred between 24 January and 27 February. The strong northerly winds were preceded by a period with unusually strong southerly winds (18 December to 24 January). These periods are indicated in Fig. 3.5, showing observations of temperature from within Kongsfjorden. The figure reveals that during winter, episodes of warm AW appeared in the deep part of the fjord basin. During the period with strong northerly winds, AW extended vertically up until it filled the whole water column. After this, a period with unusually strong heat loss to the atmosphere started, along with melting of local sea ice in the fjord or drift ice on the shelf. The end result in late April was a water column that was homogeneous in temperature and slightly stratified in salinity, very similar to the formation of ArW suggested in the previous subsection.

Wind events along the WSC can lead to geostrophic advection of AW towards Kongsfjorden as well, and Nilsen et al. (2016) published an idealized model study of this mechanism. A brief description of the mechanism is as follows: a wind curl (horizontal wind shear) adds relative vorticity to the WSC, forcing the current up or down the slope due to conservation of potential vorticity. In the case when the WSC is forced up the slope (during southerly wind events), topographic steering leads to geostrophic advection of AW into troughs on the shelf, and in some extreme situations onto the shelf itself. Results from this model study are shown in Fig. 3.6. This effect has not been tested against observations in Kongsfjordrenna. In Kongsfjorden, Inall et al. (2015) reported the mean flow in current meter data to be 4 cm s^{-1} , but with episodic events of stronger currents (see next paragraph).

Upwelling events along the WSC will in practice involve instabilities at the shelf-edge front, and will then be the ageostrophic process that Svendsen et al. (2002) mentioned. Instabilities at the shelf-edge front are laterally meandering

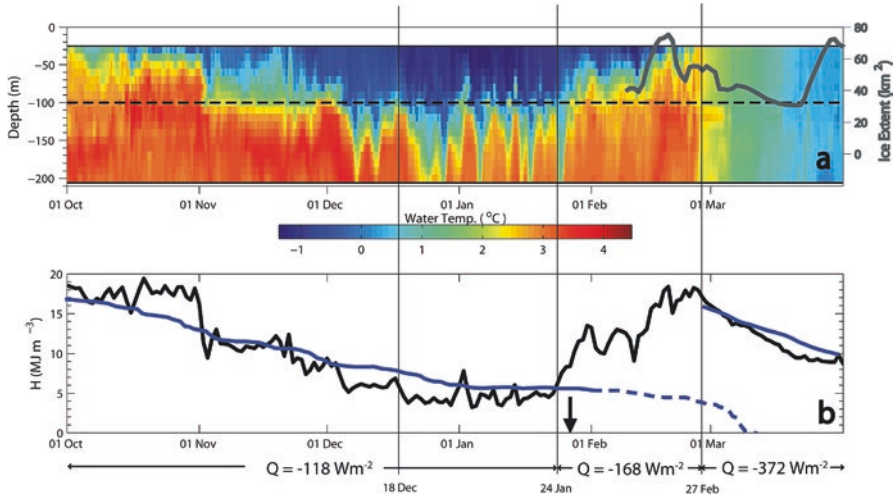


Fig. 3.5 (a) Temperature observations at Kongsfjorden mooring ($N79^{\circ}3.250'$, $E011^{\circ}18.00'$) between 30 m and 200 m with H (mean heat content) calculated over the interval 30–100 m (dashed line). The 7-day running mean of fast ice extent in Kongsfjorden is overlaid (grey). (b) Mean heat content (H) from Kongsfjorden mooring (black) and from the 1-D model (blue line – dashed when the model diverges from observations) with mean surface heat flux (Q). The model is reinitialized on 27 February 2006 and the arrow marks when the model predicts freezing. (Figure adapted from Cottier et al. (2007), their Fig. 4)

waves along the front that turn unstable and break off from the WSC in the form of eddies and filaments. The laterally meandering waves can generally be called topographic waves, and they do not always become unstable. However, even when the topographic waves are stable, they are associated with lateral exchange of heat (Nilssen et al. 2006). Moreover, stable topographic waves, generated by wind events at the shelf-edge front, can create signals that propagate along the southern side of Kongsfjordrenna towards Kongsfjorden as coastal-trapped waves with strong along-isobath currents moving back and forth over typically 2–3 days. Inall et al. (2015) detected episodes of such waves from mooring data inside Kongsfjorden (Table 3.2) with current speeds of 20–30 cm s^{-1} , and having a two-layer (baroclinic) structure with along-shore inflow in one layer concurrently with outflow in the other layer. They estimated that 100 m was a typical separation depth between the two layers. Coastal-trapped waves are trapped to steep sloping bottom, and the width of the slope and the level of stratification determine the width of their associated current. Such wave currents are in geostrophic balance and can easily be interpreted as topographically steered flow, which means that rotational constraints (Coriolis) force the flow to follow bathymetric contours. If an assumption is made that some level of mixing takes place during the inward and outward directed currents associated with these topographic waves, then the waves also contribute to the exchange of water properties between the shelf and inner fjord. Inall et al. (2015) estimated that trapped waves contribute more to exchange than either tidal

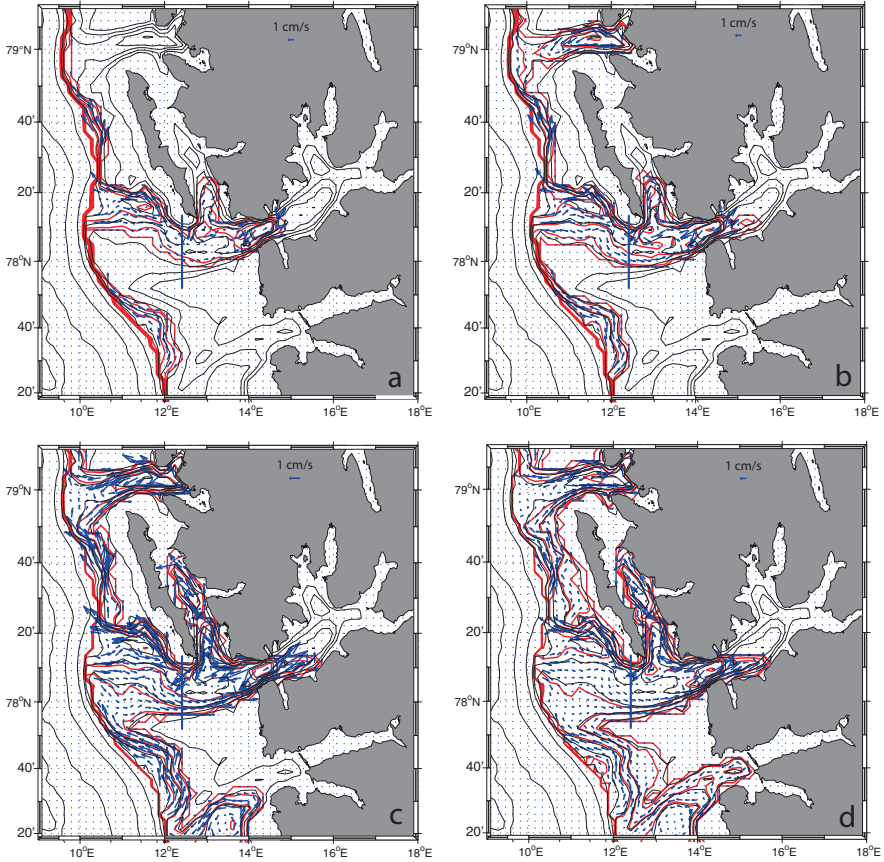


Fig. 3.6 Topographic steering of AW from the WSC in cases when the position of the West Spitsbergen Current (WSC) is shifted eastwards a distance (a) 2 km, (b) 3 km, (c) 8 km and (d) 14 km. Contoured streamlines/circulation pattern ψ (red lines) are plotted on top of the bottom topography (black lines). The blue arrows are the geostrophic velocity vectors and a velocity scale is given in the upper right corner. (Figure adapted from Nilsen et al. (2016), their Fig. 11)

or estuarine processes. The two-layer structure appearing during winter 2006 (Fig. 3.5), with layers separated at 100 m depth level, and the episodic occurrence of AW, may possibly be associated with these coastal-trapped waves. Inflow episodes of similar duration were reproduced in a recent high-resolution model study of Kongsfjorden (Sundfjord et al. 2017).

When the topographic waves along the shelf-edge front become unstable, there are two extreme versions of instabilities. The instabilities are: (1) barotropic instability (Collings and Grimshaw 1980) due to a horizontal current shear with no horizontal density gradients across the shelf-edge front, and (2) baroclinic instability (Mysak and Schott 1977) due to horizontal density gradients across a front. In practice, instabilities are likely caused by a combination of barotropic and baroclinic insta-

bilities, and other factors, like bottom features and wind, can be involved. The above mentioned upwelling situation is an example of the latter, and may actually lead to baroclinic instability at the front because deep water in the WSC is lifted upwards in the water column, altering the horizontal density gradients across the front. Instabilities in the WSC have been investigated by Teigen et al. (2010, 2011), based on current-meter time series in the WSC, linking them to generation of topographic waves in the current. As these waves are undulations of the current, they contain a strong horizontal component to the WSC, leading to transport of heat and salt across the current and shelf-edge front as the undulations develop into eddies and filaments. Typically, during a winter, there are 8–10 barotropic instability events lasting between 1 day and up to several days where interaction with surrounding local water masses occurs.

Barotropic eddies extend through the whole water column whilst baroclinic eddies extend through only part of the water column. In some cases this can imply that eddies formed by baroclinic instabilities in the relatively deep slope current (WSC) appear as barotropic eddies when they advect onto the shallower shelf. The vortex circulation of an eddy is approximately in geostrophic balance due to the large horizontal scale of these eddies (of order 10 km), in the same way as the WSC is a geostrophic current. However, their slightly ageostrophic quality determines the fate of eddies generated by the unstable topographic waves. This quality means that the eddies and filaments spread water laterally, predominantly along similar density (isopycnal diffusion), but in such a way that lighter water is eventually laid over denser water, over time leading to flattened or terrain-following isopycnals across the front (Adcock and Marshall 2000). This long-term effect is called eddy overturning, which always exchanges water perpendicular to a mean geostrophic current, and can transform a baroclinic front into a barotropic front. A barotropic front is the typical summer situation along the shelf-edge front outside Kongsfjorden (Saloranta and Svendsen 2001), perhaps leading to the misunderstanding that barotropic instability is the dominating process at the shelf-edge front. During winter, heat loss to the atmosphere is constantly increasing the density of surface water. This occurs more efficiently on the shallower shelf side of the shelf-edge front than in the deeper WSC. Continuous heat loss to the atmosphere can thus help maintain an eddy overturning because it changes the density of the water column to a different extent on each side of the front, and eddies along the front are then never able to flatten the isopycnals. Other processes that change the density of the water column, like sea ice formation and melting, can also be drivers of eddy overturning. The combined effect of wind-driven Ekman transport and eddy overturning is generally called residual-mean overturning (Marshall and Radko 2003). Tverberg et al. (2014) used such theory to explain winter evolution of the water mass on the shelf just south of Kongsfjorden.

The eddy and residual-mean overturning are not measurable circulations since eddy overturning is a slow response over weeks, as opposed to Ekman transport, which responds to the wind on a timescale of hours, and can be estimated. Evidence of eddy and residual-mean overturning is hard to specify in general circulation models, even if they have high enough resolution to resolve eddies. The method used to

quantify residual-mean overturning requires that modeled currents can be averaged both in time and along some distance of uniform bottom profile, the latter normally requiring an idealized model set up. In such an idealized model study by Tverberg and Nøst (2009), eddy activity was the only process leading to water exchange across a shelf-edge front between a shelf with water column temperature and salinity characteristics of Kongsfjorden, and a slope current with WSC characteristics. The evolution of three situations were simulated for 100 days each. Model results from an April 2002 situation, with shelf water lighter than WSC water at every depth level, had an eddy field evolving after 20 days, with eddy overturning that brought AW onto the shelf in the deep sector of the water column. An April 2007 situation, with shelf water denser than WSC water at every depth level, had an eddy field evolving after 4 days, with eddy overturning that brought AW onto the shelf at the surface. A September 2000 situation, with lighter upper shelf water and denser deepest shelf water than water at similar depth levels in the WSC, had eddies forming already the first day, with eddy overturning that brought AW onto the shelf at intermediate depth where the density across the front was the same. The eddy overturning thus appeared like a purely density-driven flow (ageostrophic). However, one should have in mind that eddy overturning is a secondary effect of the eddy activity. In the initial phase, the baroclinic eddies and filaments have a stirring effect, meaning they are stretched laterally into complex shapes, substantially increasing the area of the front between AW from the WSC and shelf water. The integrated effect of turbulent diffusion along this enlarged area, leads to an effective diffusion that can be orders of magnitude greater than the turbulent diffusion itself, depending on the degree of stretching (Marshall et al. 2006).

The shelf-edge front processes described above are summarized for a winter situation with heat loss through the ocean surface (Fig. 3.7). The surface heat loss will then drive a residual mean overturning (eddy overturning) across the shelf-edge front that will try to put light water on top of dense water. Wind forcing that will lead to Ekman transport in similar direction as eddy overturning is indicated (Fig. 3.7). During some periods, Ekman transport may of course oppose the eddy overturning. In these cases, the Ekman transport (wind) will likely lead to enhanced baroclinic instabilities, and a resulting stronger eddy overturning. Ekman and eddy overturning are the ageostrophic processes, while topographic steering governs the geostrophic advection, which involves larger volumes and will be important in all cases. The classical situation, with shelf water being less dense than the WSC, will lead to topographically-steered geostrophic advection in the deep part of the water column, while when the WSC is noticeably less dense than shelf water, the vertical extent of the geostrophic advection might be from the surface to some limited depth. Our observations indicate that when density differences across the shelf-edge front are weak, the topographic steering may involve the whole water column, and topographic steering of advected AW is pronounced. In cases when the shelf and fjord water columns are stratified, with AW occupying upper or lower part of the water column, the AW advection may also be associated with coastal-trapped wave episodes (Inall et al. 2015). Fig. 3.7 refers to three winter types, which we will define in Sect. 3.4 “Seasonal Cycle”. They are closely connected to the depth level where winter advection of AW towards Kongsfjorden occurs, and whether it enters the fjord basin.

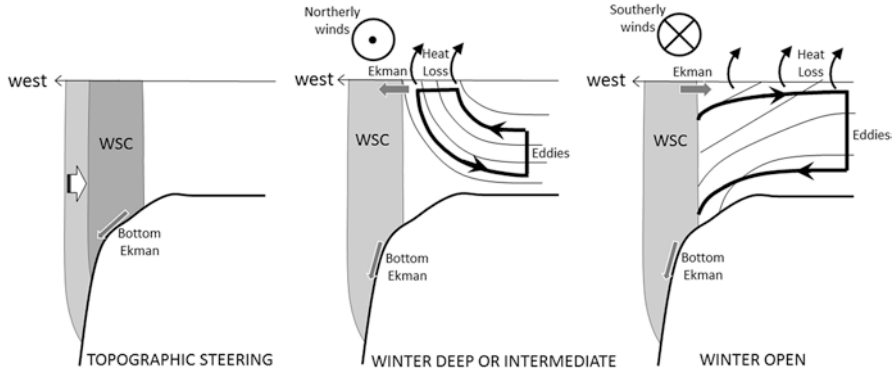


Fig. 3.7 Shelf edge processes that leads to advection of Atlantic Water (AW) towards Kongsfjorden, from the West Spitsbergen Current (WSC), inspired by Fig. 2 in Tverberg et al. (2014). Ekman refers to surface Ekman drift towards the fjord due to southerly winds or surface Ekman drift towards the ocean due to northerly winds. Thick lines (tagged with ‘Eddies’) superimposed on thin lines (isopycnals) refer to a long-term mean overturning resulting from eddy activity along the shelf-edge front, acting to put light water on top of dense water. If special wind conditions lift the WSC higher up on the shelf slope, AW will be topographically steered towards Kongsfjorden along the southern side of Kongsfjordrenna

3.3.4 Geostrophic Control

The Cottier et al. (2005) study suggests that geostrophic control at the fjord entrance prevents AW from entering the fjord during the winter season because the water column inside the fjord basin is denser than the water column on the shelf. This concept of geostrophic control was introduced by Klinck et al. (1981) to explain how a coastal current can be prevented from entering the adjacent fjord, and instead passes by the mouth of the fjord. The underlying principle is that density differences between the fjord water column and the adjacent shelf has a thermal-wind effect on the geostrophic coastal current. Thermal wind makes the geostrophic current speed decrease or increase with depth depending on the density difference on both sides of the current. If the water is lighter on the right side of the current, when facing the current direction, the current speed will decrease with increasing depth. If the situation is opposite (denser water to the right), the current speed will increase with increasing depth. The implication of this for the coastal current outside the fjord entrance is that during a winter with strong winter convection in the fjord, and the deep fjord water being denser than shelf water, the speed of the coastal current will be enhanced towards the bottom. This blocks the advection of AW into the fjord, and instead the advected AW will join the coastal current and make a detour in the mouth region. After the onset of the summer season, the density of the fjord water column gradually decreases, altering the density differences between the fjord and the shelf. When there is density matching inside and outside the fjord the geostrophic control breaks down and AW can enter the fjord at depth. Atlantic Water entering the fjord may happen during the winter as well, if the water column in the fjord has lower

density than the shelf. The speed of the coastal current will then decrease with depth, and it is possible in these situations that the coastal current is confined to an upper layer. There may then be no geostrophic control at the mouth in the deep layer, and AW can enter the fjord in that deeper part of the water column.

Klinck et al. (1981) assumed that the fjord entrance is narrow compared to the internal Rossby radius of deformation. This is normally not the case for Kongsfjorden, which should allow for baroclinic flow through the fjord entrance. Kongsfjorden is about 10 km wide, while a typical summer internal Rossby radius is 3–4 km (Svendsen et al. 2002). However, Cottier et al. (2005) observed in a numerical modeling experiment, that a geostrophic control mechanism took place at the common entrance of Kongsfjorden and Krossfjorden. Atlantic Water was advected towards the fjord along the southern side of Kongsfjordrenna, but was forced to make a detour at this entrance. Geostrophic control has also been used to explain why AW does not enter Isfjorden because it is blocked by the coastal current passing very close to the mouth of the fjord (Nilsen et al. 2008). We are not aware of any study that has focused on the path of the coastal current as it flows past Kongsfjorden, and due to the fact that the coastal current continuously interacts with the WSC and has to pass the island Forlandet along its path between Isfjorden and Kongsfjorden, the situation may be more complicated for Kongsfjorden than for the case of Isfjorden. Nevertheless, we here make the assumption that Kongsfjorden behaves somewhat similar to Isfjorden, and geostrophic control applies. Our hydrographic data indicate that the geostrophic control may happen either at the common mouth of Kongsfjorden-Krossfjorden (Kb0) or at the entrance of Kongsfjorden (Kb1).

3.3.5 *Internal Circulation*

Along the West Spitsbergen coast, the tide travels as a transient Kelvin wave (Gjevik and Straume 1989), and the tide inside the Kongsfjorden-Krossfjorden system is a response to this tidal elevation of the ocean surface outside the fjord (Svendsen et al. 2002). Tidal analysis of mooring data reveals that the tide in Kongsfjorden is dominated by three semidiurnal constituents, M2, S2, and N2, and one diurnal constituent, K1. All other constituents are very small compared to these. M2 is the most significant tidal component (Table 3.3), with the largest amplitude in both sea level elevation and in current, and the highest Signal to Noise Ratio (SNR) of all the constituents. The tidal current is however very weak and not strong enough to dominate the flow pattern. Very little of the total variance in the velocity time series is of tidal origin. Inall et al. (2015) found that these four constituents only captured 1.2% of the total velocity time series variance. Harmonic tidal analysis on the data from the three current meters in Table 3.3 showed that the tide was responsible for only 1.3%, 1.2%, and 1.2%, respectively for the three depths, of the total variance of the velocity, which is consistent with the result of Inall et al. (2015).

M2 has an amplitude of nearly 0.5 m while S2 and N2 together have an amplitude half this. The diurnal component K1 gives only a minor contribution. This

Table 3.3 Harmonic tidal analyses made from both current (left side) and pressure (right side) data from instruments at 37, 121, and 216 m at Mooring H1 for the period Sep 2014-Aug 2015

37 m	Frequency	Major (cm s ⁻¹)	Minor (cm s ⁻¹)	SNR	37 m	Amplitude (dbar)	SNR
M2	0.0805	0.814	0.024	15	M2	0.48	2900
S2	0.0833	0.307	-0.014	2.6	S2	0.16	290
N2	0.0790	0.08	0.029	0.33	N2	0.09	84
K1	0.0418	0.127	-0.037	0.34	K1	0.06	180
121 m					121 m		
M2	0.0805	0.518	0.11	5	M2	0.48	2700
S2	0.0833	0.133	0.043	0.42	S2	0.16	290
N2	0.0790	0.074	-0.054	0.29	N2	0.09	89
K1	0.0418	0.2	0.028	1	K1	0.04	140
216 m					216 m		
M2	0.0805	0.443	0.03	11	M2	0.45	470
S2	0.0833	0.143	-0.027	2.4	S2	0.14	49
N2	0.0790	0.08	-0.018	0.63	N2	0.07	10
K1	0.0418	0.094	-0.02	0.72	K1	0.05	13

The mooring's position was N78°58' and E011°58'
SNR signal to noise ratio

explains why the tide is semidiurnal in Kongsfjorden. The solar component (S2) causes the amplitudes to vary considerably during a fortnightly spring-neap period. The average difference between high tide and low tide in Kongsfjorden is about 1 m. The resulting M2 tidal ellipses from the different moorings are shown in Fig. 3.8a. The ellipses closest to land (U1, D3-D5 and H1) are nearly unidirectional, and more open away from the coast (D1/D2). In the mouth area (D1/D2), the tidal signal is stronger than further into the fjord (see Table 3.4). Mean currents from the same mooring data are shown in Fig. 3.8b. Based on topographic steering (Nilsen et al. 2016), and a relatively small internal Rossby deformation radius (3–4 km during summer, according to Svendsen et al. (2002), one would expect the circulation in Kongsfjorden to describe exactly this inflow along the southern shore that turns northwards along Blomstrandhalvøya (Fig. 3.1b) and outflow along the northern shore. The coastal-trapped waves (Inall et al. 2015) will periodically constitute a similar circulation and the reverse, similar to the tidal currents in the fjord as well, but with longer periods (2–3 days) and stronger velocity (20–30 cm s⁻¹).

Unpublished shipboard ADCP observations as well as model results sometimes reveal a semi-permanent closed eddy in this central basin of Kongsfjorden. ADCP observations during the April 2002 cruise indicated that the semi-permanent eddy was present (Cottier et al. 2003), superposed on the temperature field at 30 m depth. This particular occurrence appeared to have an eddy confined to the upper layer, and might represent a situation with restricted exchange with the shelf due to geostrophic control at the fjord entrance. A somewhat similar example of modeled circulation is shown in Fig. 3.9b. Sundfjord et al. (2017) found that such eddy patterns

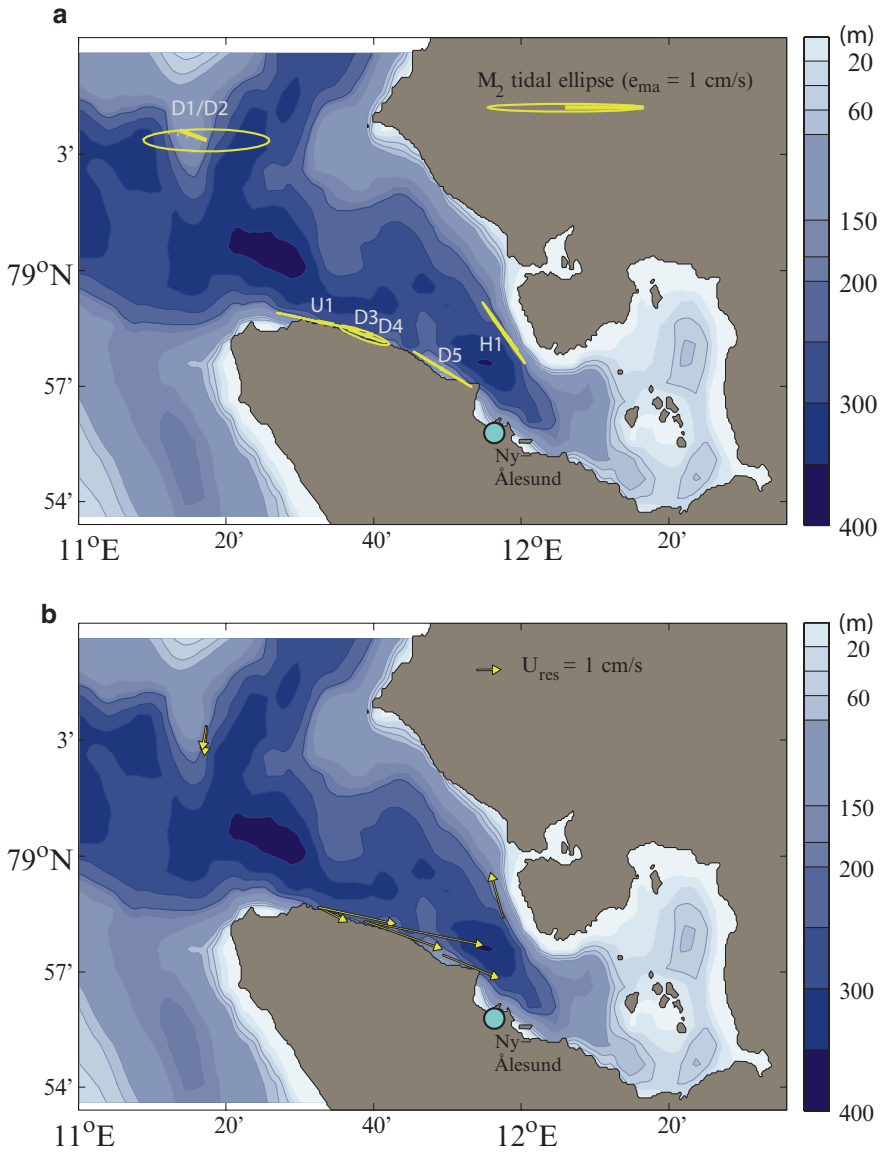
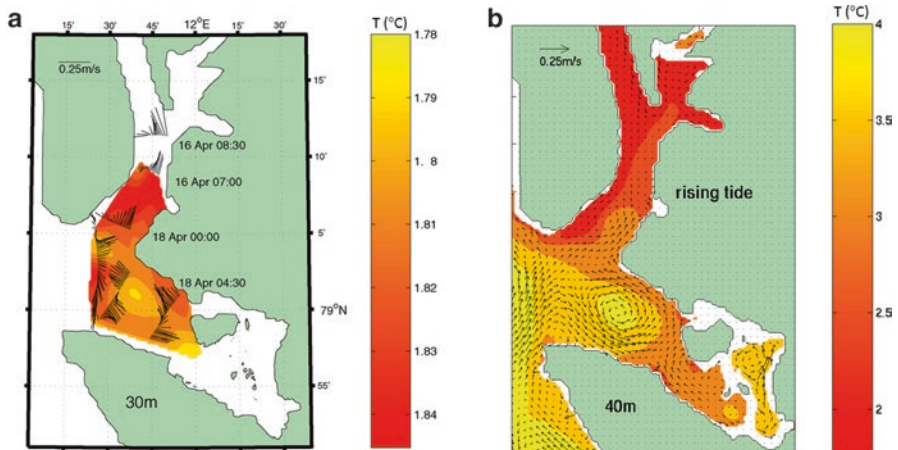


Fig. 3.8 (a) The M_2 tidal ellipses and (b) residual mean currents in Kongsfjorden from different current meter moorings as indicated in (a) and listed in Table 3.2. The mean residual current vectors at the U1 mooring are shown for both 44 m ($\sim 1.5 \text{ cm s}^{-1}$) and 97 m ($\sim 3.5 \text{ cm s}^{-1}$) depths, while the others show the depth-averaged residual currents. The time means of the residual currents are over the measuring period for each mooring

Table 3.4 Percent total variance predicted, from the tidal analyses from SAMS moorings (D1 to D5) and UNIS/GFI moorings (U1 and H1)

Moorings	Depth (m)	Total var.	Pred var.	%
D1	145–29 in 4 m bins	25.70	1.67	6.5
D2	145–29 in 4 m bins	14.99	1.76	11.7
D3	120–50 in 4 m bins	25.04	0.26	1
D4	126–62 in 4 m bins	42.86	0.89	2.1
D5	132–20 in 4 m bins	33.72	0.46	1.4
U1–1	44	25.89	0.74	2.9
U1–1	94	68.98	2.20	3.2
U1–2	94	45.69	0.93	2.5
H1	37	28.27	0.34	1.3
H1	121	11.27	0.14	1.2
H1	216	9.19	0.11	1.2

**Fig. 3.9** (a) Observed and (b) modeled snapshots of typical circulation in Kongsfjorden. (Figure adapted from Cottier et al. 2003)

in the fjord could be associated with inflow of AW as well, with periodicity similar to the coastal-trapped waves (Inall et al. 2015).

3.3.6 Fjord Ice

The extent of the sea ice cover in Kongsfjorden varies significantly between years, and the inter-seasonal evolution is highly variable (Pavlova et al., Chap. 4). Systematic mapping of sea ice cover in Kongsfjorden was established in 2003 (Gerland and Renner 2007), based on observations from the mountain Zeppelinfjellet near Ny-Ålesund at the southern shore of the fjord (Fig. 3.1b). From 2004 onwards,

there were sufficient observations to represent the inter-annual variability by e.g. the average ice covered area from all observations done within one particular month. The area is calculated from digitized maps using ArcGIS tools. The area of landfast ice in Kongsfjorden for each March during 2004–2015 show a variable but declining sea ice coverage (Fig. 3.10). The total surface area of Kongsfjorden (east of $11^{\circ}12'E$ and south of $79^{\circ}5'N$) is in comparison about 275 km^2 , and the surface area inside of the Lovénøyane (Fig. 3.1b) is $60\text{--}70 \text{ km}^2$. This implies that only in 2004, 2009 and 2011, did the ice cover extend beyond the area inside of Lovénøyane. These islands in the inner part of Kongsfjorden restrict the local circulation to such a degree that there may be distinctly more Arctic water masses inside them, than in the central Kongsfjorden basin, due to glacial runoff and ocean-glacier front interaction. The more regular fast ice cover inside Lovénøyane is an indication of this (see e.g. MacLachlan et al. (2007)).

Brine release during ice formation can be a potential contribution to the production of dense winter water. The release is strongest during the early phases of ice freezing (Notz and Worster 2008). Under land-fast ice, the ice growth becomes slower as the ice thickness increases, since ice and snow insulates the water column from the cold air above. The areal extent of open water at freezing temperatures, leading to newly formed ice, thus determines to a large degree how much brine is added to the water column (Nilsen et al. 2008). The smallest salt increase estimated for Isfjorden was in 2004 (Nilsen et al. 2008), analogous to the maximum seen in Kongsfjorden that year (Fig. 3.10), and we note that this was related to the reduced polynya area and a maximum in fast ice area.

3.3.7 *Runoff and Freshwater from Glaciers and Land*

During summer, freshwater and sediment discharges at the base of the glaciers can be significant and provide a driving mechanism for exchange of water masses with the central basin (Salcedo-Castro et al. 2013; Kimura et al. 2014; Lydersen et al. 2014). More than 80% of the land area drainage into Kongsfjorden is covered by glaciers, and therefore glacier runoff accounts for the majority of the freshwater entering the fjord. Arctic river runoff has a strong seasonality; similarly, the onset of glacier surface melt typically occurs in late spring, with peak discharges as late as July and August. This is due to the internal hydrology of the glaciers, where the initial pulse of surface melt first refreezes in the cold snow and firn until temperatures are brought to the melting point, after which the meltwater finds its way to the base of the glacier and down toward the glacier front. There it typically enters the fjord through one or a few large tunnels at or near the base of the glacier front, i.e. some 10s of meters below the sea surface. Radar measurements of ice thickness reveal that the tidewater glacier fronts in the inner part of Kongsfjorden are ca. $50\text{--}100 \text{ m}$ deep (J. Kohler, NPI, unpubl. data.). The glacial discharge released at depth is very buoyant with respect to the ambient water, and quickly rises,

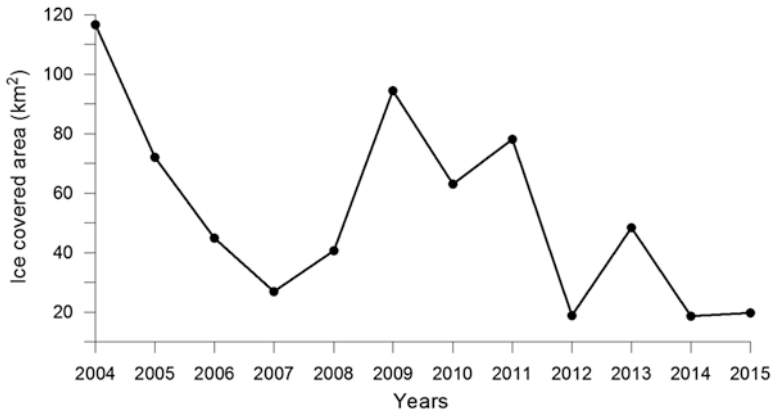


Fig. 3.10 Average fast-ice covered area in Kongsfjorden during March 2004–2015, based on photographic observations from the mountain Zeppelinfjellet, Ny-Ålesund

entraining and mixing with large volumes of surrounding water. The effects of subglacial discharge on local circulation can be profound, with large volumes of water drawn from intermediate depths and a thick, brackish outflow layer at the surface (Urbanski et al. 2017). This process is different from typical surface river runoff, which occurs in the surface layer and does not entail large conversion of potential energy into mechanical mixing. In Kongsfjorden, studies show that the modification of such a subsurface plume through mixing occurs very close to the glacier face so that its signature is not seen in the ambient water within 2 km of the glacier (MacLachlan et al. 2007). In addition to melt water drainage, the glaciers also contribute freshwater via icebergs (mostly in summer) and through frontal melt (potentially the whole year) (Luckman et al. 2015). Frontal melt will be strongly related to the heat content of the surface and intermediate layers; in years where AW protrudes deep into the fjord and relatively high in the water column, frontal melting is likely to be largest (Luckman et al. 2015).

Local winds, usually blowing along the fjord axis move the surface layer, typically so that wind blowing out of the fjord forces freshwater to concentrate along the northern shore and flow out of the fjord (Ingvaldsen et al. 2001). Such outflow would be compensated by inflow of more saline, warmer AW over the bottom, along the southern shore (Moffat 2014). This wind-driven circulation may enhance glacier melting, increase freshwater discharge thus generating a feedback that will force more intensive water exchange. A high-resolution model study by Sundfjord et al. (2017) shows significant transport of water towards the glacier fronts in the inner part of the fjord, throughout the annual cycle. In that study, wind appears to be the primary driver of variability for this circulation. It has been shown that Van Mijenfjorden (Fig. 3.1a), which has similar width to Kongsfjorden, responds rapidly to changes in wind forcing; a shift from down-fjord to up-fjord wind can move the thickest segment of the fresh surface layer from the northern to the southern side in a matter of hours (Skarðhamar and Svendsen 2010).

3.3.8 *Vertical Structure and Mixing*

We have argued that the vertical density structure and the density difference between the water column in the fjord and on the shelf controls the depth of inflow of AW to the fjord. However, we have also noted that topographically-steered advection along the southern shore, combined with bursts of intensified flow due to coastal trapped waves, are likely to be responsible for the largest volumes of inflow of AW. The apparent advection of AW at particular depth levels can then be explained by the eddy stirring effect spreading water along isopycnals away from the core of a geostrophic flow, which can either be the flow along the shore inside Kongsfjorden or the WSC, or a combination of these. The stirring effect of eddies and filaments behave like isopycnal diffusion, or simplified, like horizontal diffusion. Vertical or diapycnal diffusion adds to this by changing the stratification (vertical stability) of the water column and may be essential in the slow process of reducing the density of the Kongsfjorden water masses after the winter.

The most striking feature in terms of vertical stability is the seasonal pycnocline, which for all practical purposes isolates the deeper layers from the otherwise efficient wind mixing. Wind energy will be able to deepen the mixed layer during strong wind events, but it will not erode further into the seasonal pycnocline as the density difference is too large between surface and deeper waters. During autumn and winter, wind driven mixing will more efficiently aid in breaking down stratification as the water column is cooled from the surface and the freshwater content decreases with the cessation of melt water supply. Tides and other persistent currents may contribute to vertical mixing if they are sufficiently strong, especially over shallow or steep topography and in interaction with significant density gradients. In Kongsfjorden, we have observed that tidal currents are weak (Fig. 3.8a), and the mean internal circulation in the fjord as well (Fig. 3.8b). We see a need for more investigation of the temporally and spatially varying rates of diapycnal mixing in the fjord, especially during periods where the geostrophic control prevents advection of AW into the fjord. Knowledge of diapycnal mixing rates inside the fjord can indicate how fast the internal fjord processes can contribute to the preconditioning of the water column that is required to initiate exchange of AW with the shelf and slope.

3.4 Seasonal Cycle

Svendsen et al. (2002) deduced a scenario for the mechanisms governing the production of water masses in Kongsfjorden, solely based on summer temperature-salinity (TS) characteristics. The established scenario is as follows: In autumn and winter, the fjord water is strongly cooled at the surface through heat loss to the atmosphere, leading to densification of the surface water and convection; producing Local Water (LW). Sea ice will begin to form and brine is released when the surface layer reaches the freezing point. The combination of cooling and ensuing increase

Table 3.5 Definitions of water masses found in Kongsfjorden

Water mass	Abbreviation	T (°C)	S _P (psu)	S _A (g kg ⁻¹)
Atlantic water	AW	3.0–7.0	34.9–35.2	35.1–35.4
Transformed Atlantic water	TAW	1.0–7.0	34.7–34.9	34.9–35.1
Surface water	SW	1.0–7.0	30.0–34.0	30.1–34.2
Intermediate water	IW	1.0–7.0	34.0–34.7	34.2–34.9
Local water	LW	–0.5 – 1.0		
Winter-cooled water	WCW	–1.9 – –0.5	34.4–35.0	34.6–35.2

Adapted from Svendsen et al. (2002)

S_P is in practical salinity units (psu), S_A is in absolute salinity (g kg⁻¹)

in salinity can lead to deep convection, which reaches the bottom in the fjord interior in periods with sufficient freezing; producing Winter Cooled Water (WCW). In spring, when sea ice begins to melt and the surface water is heated by solar radiation, a low-density surface layer forms. This layer ranges from a few cm when melting occurs without wind-driven mixing, to typically 10–20 m after a longer period of melt and with wind-driven down-mixing of the fresh water, or entrainment of saltier LW into the faster moving surface layer. Freshwater from glaciers and rivers will further increase the freshwater content, forming low salinity and warm Surface Water (SW). This low-density SW will increase vertical stability and will tend to flow out of the fjord. In response, and as partial compensation for this outflow, there are seasonally varying influxes of intermediate and deep AW from the WSC and coastal water (normally ArW) of intermediate salinity, typically following the southern shore into the fjord. AW and ArW will mix along their path; forming Transformed Atlantic Water (TAW); the predominant Atlantic water mass found in Kongsfjorden. Below the SW layer, there will be a transition layer called Intermediate Water (IW) that is formed through mixing with whichever water mass resides below SW in the water column (usually TAW or LW/WCW).

This seasonal cycle is typical of Arctic fjords in general (Cottier et al. 2010), where advection of water from the open ocean into the fjord is expected to be important only during summer (their Fig. 3). However, the Kongsfjorden Transect reveals that advection of AW from the WSC can be significant also during winter. Moreover, Svendsen et al. (2002) did not expect to find pure AW inside Kongsfjorden, only TAW. In recent years, such AW from the core of the WSC has indeed been observed inside the fjord during summer. We adapt the water mass classifications from Svendsen et al. (2002), as defined in Table 3.5, with AW having the characteristics of water in the WSC, as defined by Swift (1986) and Hopkins (1991). Note that we are using the old standard Practical Salinity (PSS78) in our water mass classifications, but show in Table 3.5 corresponding water mass limits in the new TEOS-10 standard; Absolute Salinity (Millero et al. 2008), calculated by the Gibbs Seawater (GSW) toolbox (McDougall and Barker 2011). Water mass salinity limits are around 0.16 psu higher in Absolute Salinity than in Practical Salinity. Cottier et al. (2005) applied a slightly different classification of water masses, adapted to conditions north of Svalbard, involving more influence from melting sea ice (Rudels et al.

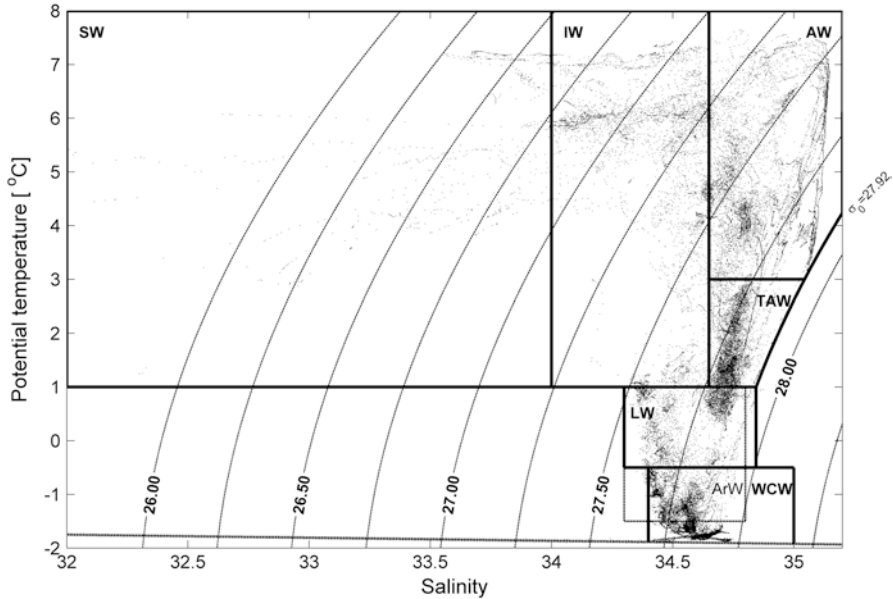


Fig. 3.11 Temperature-salinity observations from Kongsfjorden in April, June, July and September 2002, as well as September 2000, 2001 and August and September 2003. Water mass classifications differ slightly from Table 3.5. Isopycnals are at 0.25 intervals, and the dotted line indicates the freezing point. (Figure adapted from Cottier et al. (2005), their Fig. 2)

2000). Their water masses were the same as in Table 3.5, except for lower salinity limit (34.65) in both AW and TAW, as well as an upper density limit ($\sigma_\theta < 27.92 \text{ kg m}^{-3}$) for both these water masses. This limit corresponds to the density at the bottom of the AW layer in the WSC. Their notion was that water masses inside Kongsfjorden would never be denser than this unless significant sea ice formation was involved, producing denser WCW, and this implied that LW would have an upper salinity level. Our data will prove this notion to be wrong, as surface cooling of AW can produce denser winter water than the WCW classification. However, observations from the summers 2000–2003 and April 2002 all fitted well into those classifications, as can be seen in Fig. 3.11, adapted from Fig. 2 in Cottier et al. (2005).

The seasonal cycle in 2002 in the Kongsfjorden water masses, as observed by Cottier et al. (2005), agrees well with the cycle suggested by Svendsen et al. (2002). Based on mooring data, they observe that AW/TAW became present in the fjord from a certain time during summer. With limited data available, they also observed that both the timing and depth of this AW inflow could vary between summers, and proposed that the consequent ‘warm’ and ‘cold’ years are really a result of early or late onset of this AW inflow. The summer 2003 is then a good example of a late onset of AW inflow, as can be seen in Cottier et al. (2005) their Fig. 10. They linked the timing of the inflow to the breakdown of geostrophic control at the fjord entrance, and discussed that it would most likely depend on mechanisms internal to the fjord,

like freshwater runoff, surface heating, vertical mixing and wind forcing. We propose that it would also depend on the density of the Kongsfjorden water column at the start of the summer season, i.e. affected by the type of dense winter water production.

In our data, there are 11 years with what we regard as late winter observations (April–May) in the central basin of Kongsfjorden (between stations Kb2 and Kb3; Table 3.1; Fig. 3.1b). TS data from these years reveal large interannual variability in winter production of water masses in Kongsfjorden (Fig. 3.12). A typical winter production with heat loss to the atmosphere and brine release through varying rates of sea ice formation, will form a water column having close to freezing temperature through the entire column, but salinity slightly increasing with depth; a mini version of a cold halocline layer in the Arctic (Rudels et al. 1996). Only in 2002, our observations show a water column structured like this, containing WCW from surface to bottom. In April 2006 a halocline layer filled the fjord, with relatively warm temperatures in the range 0–0.5 °C, and we have suggested that this water mass may have been formed by sea ice melting combined with strong surface heat loss (see Sect. 3.3.2 “Forcing Mechanisms/Spitsbergen Polar Current”). The whole water column fits into the LW definition. The Kongsfjorden water mass in April 2006 was perhaps not formed locally, but advected into the fjord from the shelf by the coastal current. Other than in 2002, only in 2001 we observe WCW in the deepest part of Kongsfjorden, while the rest of the water column was rather warm.

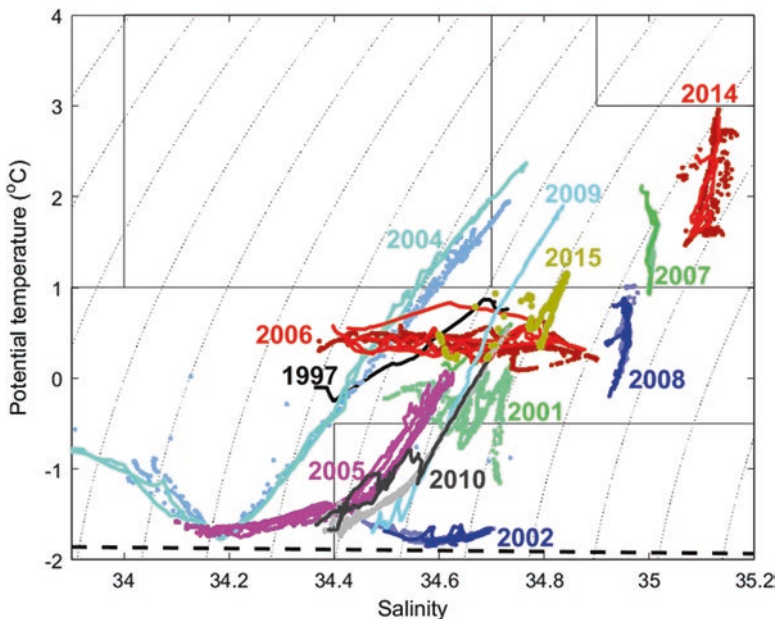


Fig. 3.12 CTD data from April or May from years indicated in plot. Solid lines are from locations in vicinity of Kb1, dots from locations in vicinity of Kb2 and Kb3. Thick dashed black graph is freezing line. Black thin lines indicate water mass classifications from Table 3.5

Section plots shown in Appendix A reveal that the rather warm water in winter 2001 was due to advection of AW across the shelf at an intermediate level.

In April 2001 (and also in April 2002), AW influence is more pronounced in the vicinity of Kb1 (Kongsfjorden entrance) than in the central basin (Kb2–Kb3). The winters 2001 and 2002 may thus be influenced by situations when AW advection is blocked at the fjord entrance due to geostrophic control and recirculates back across the shelf. These winters produce winter water that seem to involve convection to the bottom, and very limited amounts of AW entered the fjord. However, the remaining winter observations give the impression that it is common for advected AW to enter the fjord basin through the fjord entrance. This can be a significant factor that determines the water properties in late winter. The winters 2004 and 2005 were examples of this (Fig. 3.12). Atlantic Water inflow was apparent in the deepest part of the water column, while it seems that a halocline was formed down to some intermediate depth. In contrast, the AW inflows in 2007, 2008 and 2014 were pronounced at surface level. The strength and depth level of the AW advection is indicated in Table 3.6 determined by both CTD data and from mooring data (time series shown in Hegseth et al., Chap. 6).

We select 3 years, 2002, 2004 and 2007, representing the most distinct versions of the three characteristically different winter scenarios we just described. The mean winter hydrography of the Kongsfjorden Transect from each of these 3 years is shown in Fig. 3.13, as well as the summer mean hydrography from the same years. All these three winter transects are noticeably different from the winter mean calculated from the total data set (Fig. 3.2). The winter temperature mean from the total dataset has perhaps the closest resemblance to winter 2002, but is warmer. The winter salinity mean from the total data set, however, has closer resemblance to the winter 2004, but is more saline. A comparison between the single year summer means and the summer mean calculated from the total dataset (Fig. 3.3) shows discrepancies as well.

Summer observations are much more numerous and available from every year in our dataset. We observe advection of AW into the fjord every summer, where AW gradually mixes with the winter-produced water masses present in the fjord. This implies that the AW content gradually increases during the summer, while winter-water content decreases. However, the winter water mixed with AW is still detectable even late in the summer season. Based on all available summer data and comparison with the winter data (Fig. 3.12), we suggest that summer hydrographic profiles in Kongsfjorden form three different characteristic shapes in the TS diagram, depending on which type of winter production has been dominating. In the following, we point to some characteristic differences between three types of seasonal cycles in hydrography of the Kongsfjorden Transect.

Winter Deep winters (resulting in summer profiles shown in TS diagrams in Fig. 3.14) is characterized by winter convection in Kongsfjorden that extends all the way to the bottom, with either no winter AW advection or limited AW advection into the fjord at some intermediate depth. Convection to the bottom as well as AW advection limited to the shelf area, are indicated in the winter 2002 section plots (Fig. 3.13). The winter profiles from 2001, 2002 and 2006 (Fig. 3.12) are examples of

Table 3.6 Number of winter stations in vicinity of Kb1 and between Kb2-Kb3 selected for plotting in Fig. 3.12, together with observation date and likely AW advection type into Kongsfjorden, preceding the observation date, and observed winter AW advection from Kongsfjorden mooring data

Year	Kb1 #	Date	Kb2-Kb3 #	Date	Likely winter AW advection	Mooring observed winter AW advection	Kb2-Kb3 #	Date	Suggested winter convection depth
1994							3	18 Sep	Intermediate
1995							4	18 Aug	Intermediate
1996							2	16 July	Intermediate
1997	1	31 May	–	–	Deep		5	16 Aug	Bottom
1998							1	14 July	Intermediate
1999							2	12 July	Intermediate
2000							8	10–12 Sep	Bottom
2001	1	19 May	4	19 May	Interm.		5	3 Sep	Bottom
2002	8	15 April	9	15 April	Weak interm.		5	27 Sep	Bottom
2003							16	2 Aug	Bottom
2004	2	4 May	3	4 May	Strong deep	Deep	7	22–23 Aug	Intermediate
2005	4	24 April	5	25 April	Deep	Deep	3	13 Sep	Intermediate
2006	4	27 April	5	25, 30 April	Interm. and melting?	Deep – no	6	20 Sep	Bottom
2007	2	29 April	3	29 April	Surface	Surface	5	9–10 Sep	Bottom AW
2008	5	19 April	3	18, 22 April	Surface	Surface	4	12–13 Sep	Bottom AW
2009	1	26 April	–	–	Strong deep	Weak – strong deep	6	12–13 Sep	Bottom
2010	2	27 April	3	28 April	Deep	Strong – weak deep	3	11–12 Sep	Intermediate
2011						Weak – strong deep	4	10 Sep	Bottom
2012						All depth	8	8–9 Sep	Bottom AW
2013						Weak surface	6	29, 31 Aug	Bottom AW
2014	2	9 May	3	10 May	Surface	Weak surface	3	30 Aug	Bottom AW
2015			1	8 May	Interm		3	15 July	Bottom
2016							3	26 July	

Number of selected summer stations in the central basin together with suggested preceding dominant winter vertical convection types; Bottom (Winter Deep, Fig. 3.14) Intermediate (Winter Intermediate, Fig. 3.15) or bottom convection of AW (Winter Open, Fig. 3.16). The selected stations are subsamples from the Kongsfjorden Transect data, with additional data provided by the Norwegian Polar Institute from July 2015 and 2016

this type, indicating that the convection can be a result of either sea ice formation (2002), or heat loss to the atmosphere, possibly combined with some sea ice melting (2006; after the massive AW advection into Kongsfjorden). The deep convection leads to dense bottom water in the fjord, forcing the summer advection of AW to occur at some intermediate depth. The depth level of AW advection, as well as location of old winter water, are indicated in the summer 2002 section plots (Fig. 3.13). Vertical mixing of this AW layer with solar-heated surface water above it leads to formation of relatively warm and saline IW.

Winter Intermediate winters (resulting in summer profiles shown in TS diagrams in Fig. 3.15) are characterized by winter convection that is limited to some intermediate depth, with winter advection of AW into the deepest part of the water column. The location of AW advection and convection for winter 2004 are indicated in the section plots in Fig. 3.13. The winter profiles from 2004, 2005 and 2010 (Fig. 3.12) are typical examples of this type, while 1997 and 2009 might be examples of years when the geostrophic control prevented AW advection in winter to enter the central basin (winter observations made only close to Kb1; see Table 3.6). The advection of AW continued to be located very deep also in summer, resulting in relatively cold water at intermediate level. The cold water was the remnant of winter water, as indicated in the section plots in Fig. 3.13 for summer 2004, together with deep inflow of AW. As can be seen in Fig. 3.15, both IW and SW were generally colder than in the Winter Deep profiles (Fig. 3.14).

Winter Open winters (resulting in summer profiles shown in TS diagrams in Fig. 3.16) are characterized by AW advecting into the fjord over depths that include the surface layer, and winter convection of this AW all the way to the bottom of Kongsfjorden. Location of AW advection, and convection for winter 2007 are indicated in the section plots in Fig. 3.13. This scenario is typical during winters with very little sea ice present in the area, and the winter profiles from 2007, 2008 and 2014 (Fig. 3.12) are examples of this type. The summer situation is then quite similar to that after Winter Deep, except that the advection of AW may be exceptionally shallow due to the very dense winter water that this type of winter production forms. In the section plots from summer 2007 (Fig. 3.13), we have indicated large amounts of old winter water, and shallow inflow of AW.

There are two additional characteristic differences between the hydrographic winter transects in Fig. 3.13, which seem to be associated with the three winter types. During a Winter Deep (2002), the WSC is narrow and confined to the shelf-edge region. Typically, the upper part of the shelf water column is less dense, while the deep part of the shelf water column is denser than the WSC, and we observe little exchange across the front. During a Winter Intermediate winter (2004), the WSC tends to be isolated from the surface, meaning that shelf water spreads westward on top of the WSC. We have indicated this westward spreading of shelf water in Fig. 3.13. The advection of AW from the WSC onto the deep part of the shelf water column is extensive, and the WSC is clearly denser than the shelf water at all depths. During a Winter Open winter (2007), the WSC reaches the surface and is generally less dense than the shelf water in the whole water column, and we observe a pronounced advection of AW in the upper part of the water column. These frontal

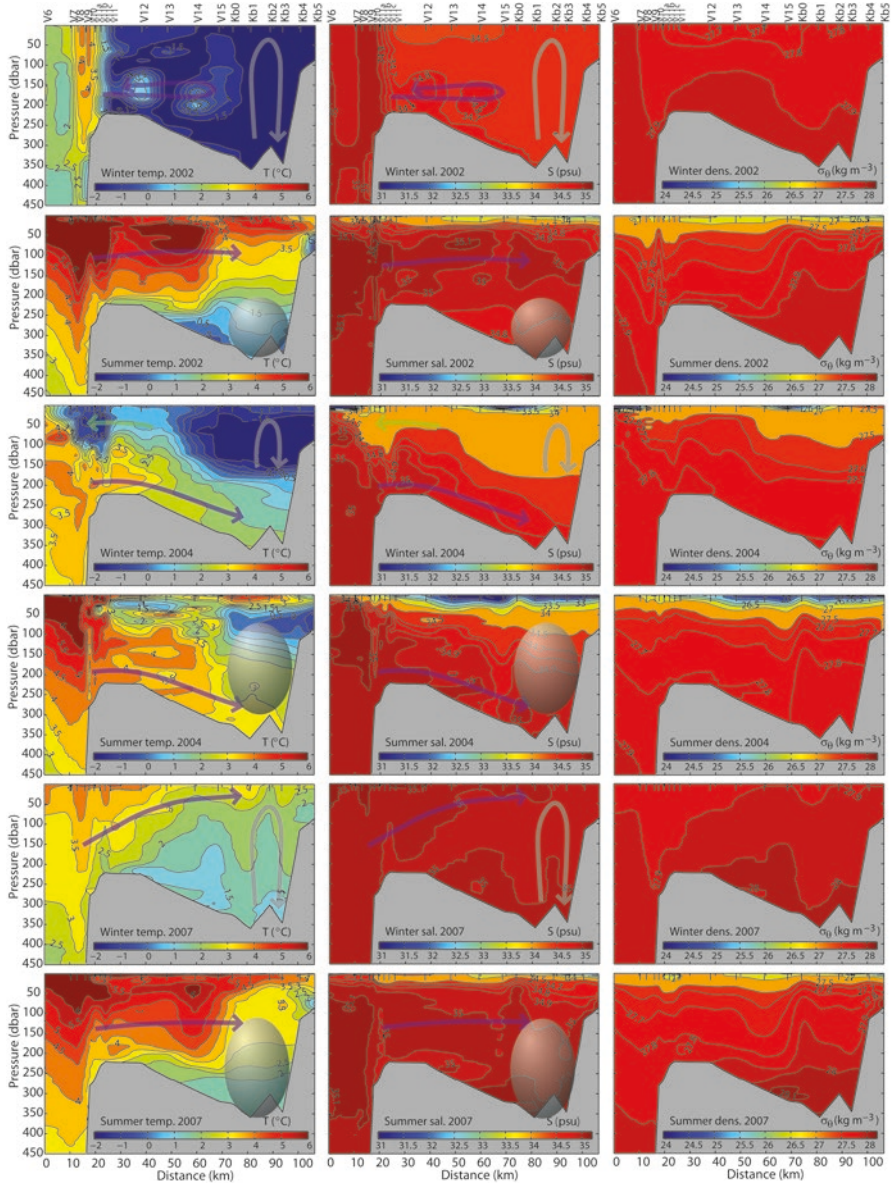


Fig. 3.13 Mean winter and summer temperature, salinity and potential density along the Kongsfjorden transect, based on all available Kongsfjorden Transect data in 2002 (having “Winter Deep” winter), 2004 (having “Winter Intermediate” winter) and 2007 (having “Winter Open” winter). Purple arrows indicate path of main inflow of AW. Green arrow indicate surface off-shelf flow of shelf water. Gray arrows indicate winter convection depth in Kongsfjorden, and spheres indicate location of old winter water

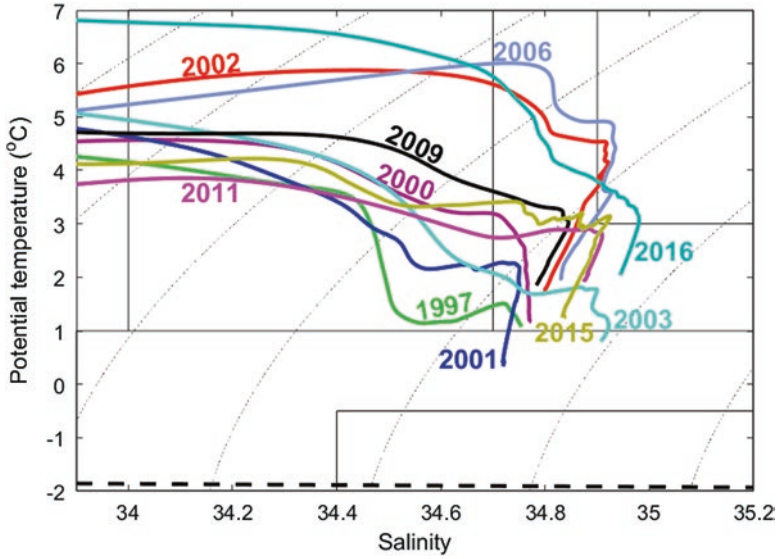


Fig. 3.14 Examples of summer mean temperature-salinity-profiles from Kongsfjorden central basin (between Kb2 and Kb3) after what we suggest is a “Winter Deep” winter with convection all the way to the bottom and no advection of AW into the central basin. Refer to Table 3.6 for dates of and number of observations

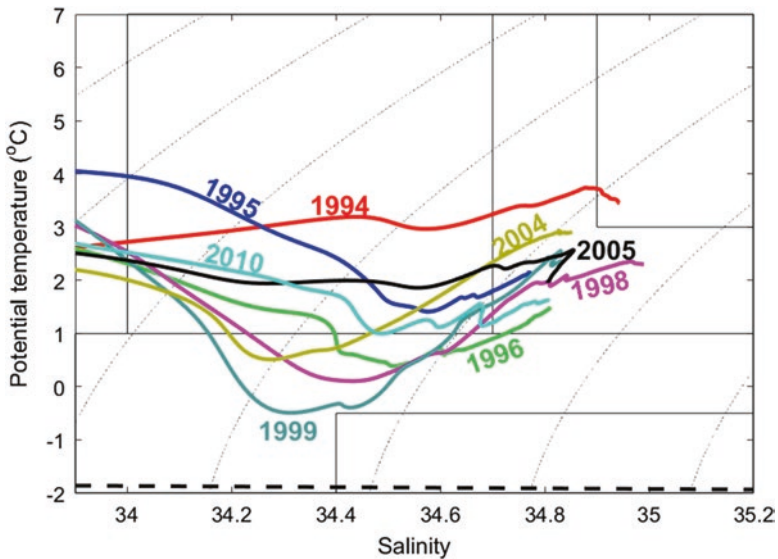


Fig. 3.15 Examples of summer mean temperature-salinity-profiles from Kongsfjorden central basin (between Kb2 and Kb3) after what we suggest is a “Winter Intermediate” winter with convection only to some intermediate depth, and advection of AW into the central basin in the bottom layer. Refer to Table 3.6 for dates of and number of observations

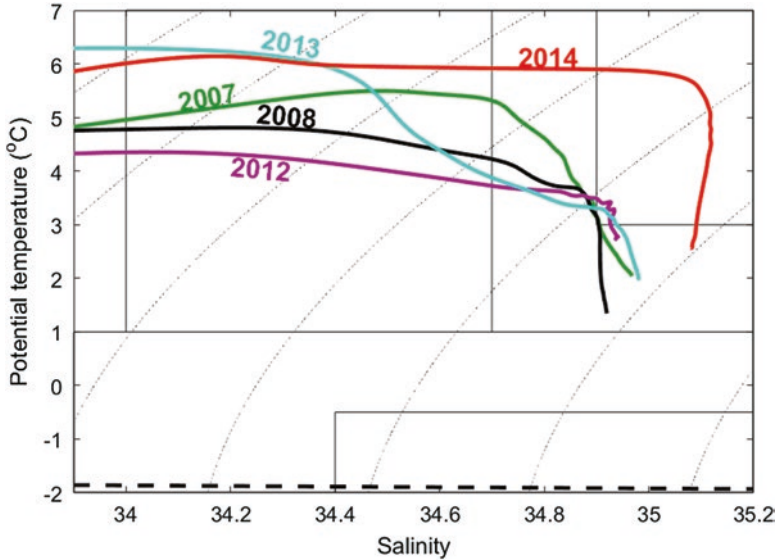


Fig. 3.16 Examples of summer mean temperature-salinity -profiles from Kongsfjorden central basin (between Kb2 and Kb3) after what we suggest is a “Winter Open” winter with advection of Atlantic Water (AW) into the central basin in, or including, the surface layer, and convection all the way to the bottom. Refer to Table 3.6 for dates of and number of observations

exchange behaviors all agree with expected eddy overturning (Tverberg and Nøst 2009). However, topographically-steered geostrophic advection of AW is an additional factor, which may be particularly strong in situations when density differences across the shelf-edge front are weak. The winter 2014 was an example of such a situation, resulting in a winter water column in Kongsfjorden where we observed TS characteristics closest to the AW type (see Fig. 3.12).

The second characteristic difference between the hydrographic winter transects in Fig. 3.13 were associated with our assumption that geostrophic control at the fjord entrance prevents AW from entering the fjord only when the fjord water is denser than the shelf water. The Winter Deep type of winter somewhat confirms this, as it seems to have a less dense water on the shelf just outside the fjord entrance, which might be associated with geostrophic AW advection making a detour at the fjord entrance. Winter Intermediate winters seem to be associated with a water column in Kongsfjorden interior that has lower density than the shelf, and free entrance of AW in the deep part of the water column. Observations from Winter Open winters are few, but density differences across the fjord entrance seem to be weak in those available, apparently leading to strong topographically-steered geostrophic advection of AW into Kongsfjorden. We do not expect that the density differences between the fjord and shelf water columns are stationary throughout each winter, so we may for instance expect that geostrophic control break down during segments of Winter Deep winters.

The standard view of the seasonal cycle of stratification in an Arctic fjord includes the Winter Deep, with sea ice formation as an important process, as illustrated in a review on Arctic fjords by Cottier et al. (2010). In light of the varying mechanisms involved during winter formation of water masses in Kongsfjorden in particular, we include here an updated version of their illustration of the seasonal cycle (Fig. 3.17). We propose that the main impact of the three different winter types on the summer water mass situation is that the core of summer AW advection will occur at varying depth levels. However, every summer we see remnants of winter water in the fjord (old winter water in Fig. 3.17) that is more or less influenced by winter AW advection. The depth level of the summer AW advection will depend largely on the density of this old winter water; the denser it is, the shallower is the summer AW advection. To a large degree, we may expect that Winter Open winters will produce the densest winter water, while Winter Intermediate winters will produce the least dense. However, there are large variations, and the depth level of AW advection at all times in the seasonal cycle will depend on external forcing mechanisms as well; on the shelf, in Kongsfjordrenna and at the shelf-edge front inshore of the WSC, in addition to the geostrophic control that can limit exchange at the fjord entrance. Given the large variations, both seasonally and between years, it is important to study each year separately when trying to interpret which forcing mechanisms have been important for shaping the hydrography of the Kongsfjorden Transect that particular year. We have sufficient data coverage to form 32 annual versions of winter or summer hydrography of the Kongsfjorden

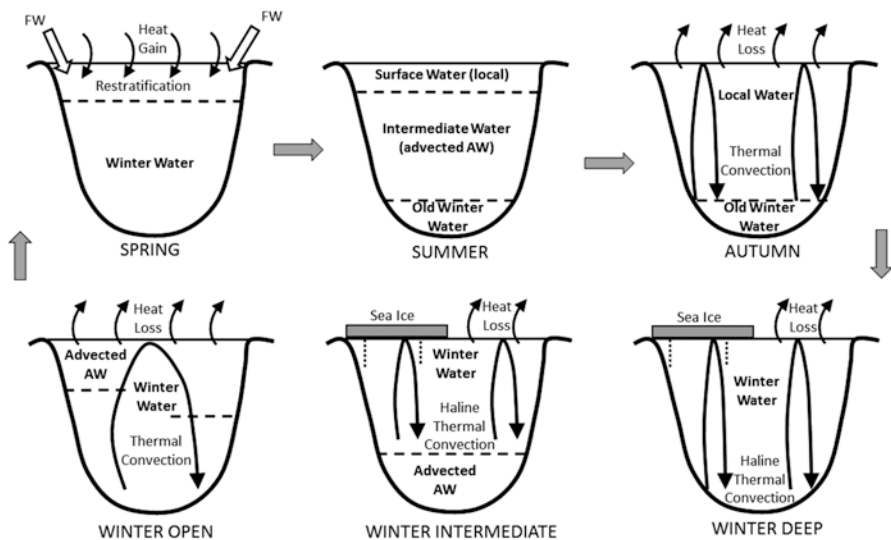


Fig. 3.17 Illustration of the seasonal cycle of stratification in Kongsfjorden, modified from Fig. 3 in Cottier et al. (2010). See text for explanation of types of winters. Sea ice influence can be extracting (during freezing) or adding (during melting) freshwater, in addition to freshening due to the seasonal ice melt in spring

Transect; the 13 winters averaging into Fig. 3.2 and the 19 summers averaging into Fig. 3.3. All are shown in Appendix A, grouped into which types they are most likely associated with.

3.5 Inter-annual Variability of AW in Kongsfjorden

We have shown that both the seasonal and inter-annual variability in the Kongsfjorden water masses can be substantial, and that this is largely due to the varying influence of AW from the WSC. Mooring data uniquely provide a continuous annual measure of water temperatures and we use these to construct an index that quantifies the relative proportion of AW present in the system. The index is based on the temperature from all loggers located in the depth range 70 m to the bottom (to reduce bias by any surface heating). Data are restricted to the 3-month period of August to October, which typically shows the greatest occupation of the fjord by AW. Atlantic Water was identified in the data as having a temperature $>3\text{ }^{\circ}\text{C}$ and the index is calculated by multiplying the mean temperature of AW by the % occupation determined from the depth distribution of water $>3\text{ }^{\circ}\text{C}$. The index anomaly (based on the full period of mooring observations) illustrates the variability among years (Fig. 3.18). The AW

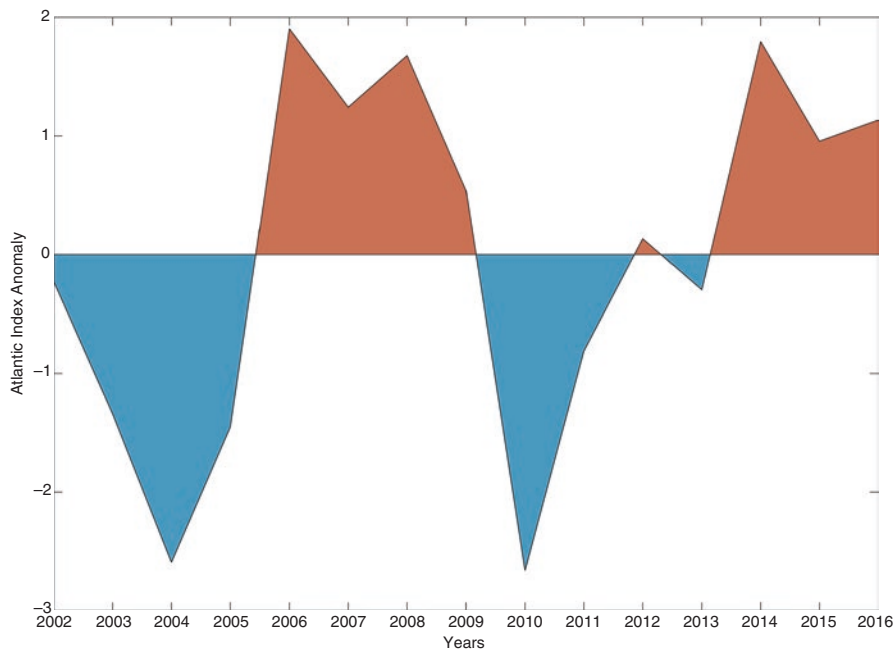


Fig. 3.18 Atlantic Water Index Anomaly for 2003–2012, based on temperature loggers between 70 m and ca 200 m depth on the Kongsfjorden mooring. Each year represents the mean temperature from these loggers during three summer months; July–September

index potentially provides a tool for systematic comparison (e.g. correlations) between oceanographic, meteorological, glacial and biological time series.

Our Kongsfjorden Transect data set provides salinity data in addition to temperature data. Moreover, since AW is normally both the most saline and warmest water mass in the region (disregarding solar heating of surface water), examining inter-annual variations in temperature and salinity may be an alternative way to express the AW influence. Average temperatures and salinities based on this data set are presented in Fig. 3.19, with additional data from July 2015 and July 2016. We present both available winter (January–May) and summer (July–September) averages, and expand the time series backwards to 1980, to better detect trends. The values are based on stations with bottom depth deeper than 100 meters, and the averaging is made as a weighted average, where the value for each depth level is multiplied by

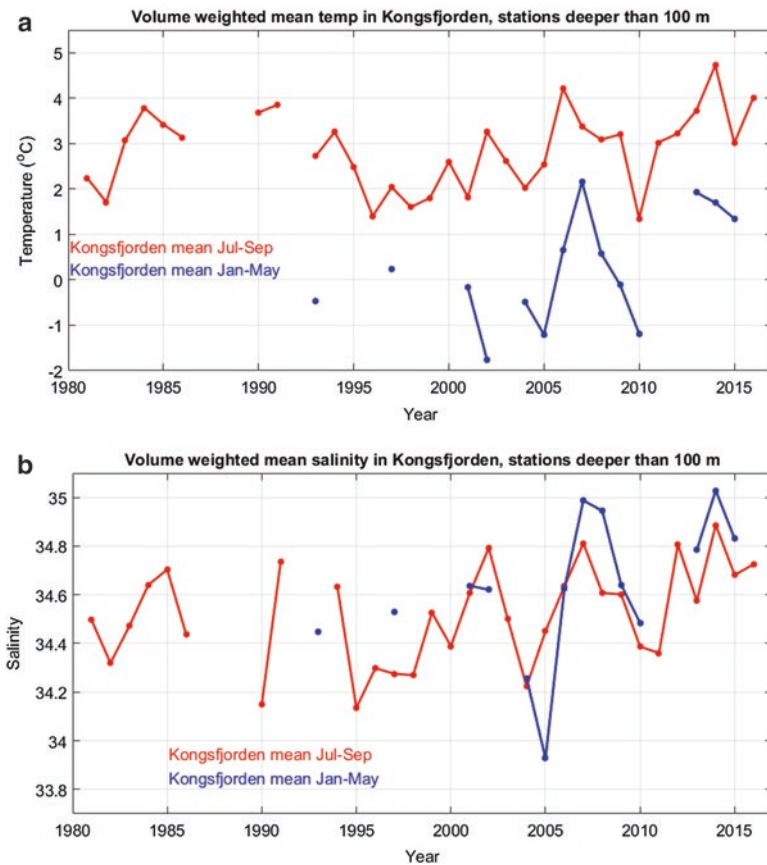


Fig. 3.19 (a) Time series of volume-weighted mean temperature (i.e. temperature value for every meter in the water column is weighted with horizontal fjord areal extent at that depth). Only CTD stations sampled in Kongsfjorden with bottom depth >100 m have been included in the averaging. (b) Similarly for salinity

the area of Kongsfjorden at that depth level, and the sum of all these is divided by the total volume of the fjord. This method makes the values represent the total heat and salt content in the fjord, and in that sense differ from the simple averaging method for the AW index (Fig. 3.18), as well as in an earlier version of temperature and salinity time series from Kongsfjorden, published in Tverberg et al. (2008).

The Atlantic Index derived from the mooring data (Fig. 3.18) gives a more robust measure of AW content since it is based on data collected continuously throughout the summer, while the CTD temperature means (Fig. 3.19a) would be biased by cold water appearing in the water column, as well as the varying timing of the CTD surveys on which they are based. We deduce from the extended CTD time series (Fig. 3.19) that we cannot extract a definite trend in summer values. Although we can say that 2006–2007 and 2014 had the warmest and most saline summer water masses in the fjord, we note that during the 1980s and around 1990 there were almost equally warm and saline summer water masses in the fjord. The winter values however, appear to be extremely high in 2007 and 2014 (temperature and salinity combined), which coincides with winters with very little drift ice on the West Spitsbergen Shelf. The mean AW core temperature in the WSC outside of Kongsfjorden varies from 3.6 °C to 4.4 °C in summer (Fig. 3.4a) and is always higher than the mean summer temperature in Kongsfjorden (Fig. 3.19a). However, the difference varies from year to year, as we would expect since the amount of AW advecting into the fjord depends on several factors, as we describe under Sect. 3.3 “Forcing Mechanisms”.

Based on the same Kongsfjorden Transect data that we used to calculate the averages in Fig. 3.19, we have constructed the vertical distribution of summer water masses in the total volume of Kongsfjorden, as a time series (water masses as defined in Table 3.5; Fig. 3.20). The interaction between winter and summer that we proposed when we defined the winter types, can be used to explain the inter-annual variations in vertical distribution of water masses. The last half of the 1990s was generally characterized by Winter Intermediate winters (Fig. 3.15) leading to deep summer inflow of AW and cold upper layer, with 1997 as a possible exception. The early part of the 2000 decade was generally associated with Winter Deep (Fig. 3.14) leading to cold deep water and shallower summer AW advection. The typical summer distribution after a Winter Open winter (Fig. 3.16) is also clearly apparent with AW and TAW influence in most of the water column and rather shallow summer AW advection (years 2007–2008 and 2012–2014). We include also the volume fraction of AW+TAW present in the fjord each summer. During the overlapping period, the AW+TAW fraction variation (Fig. 3.20) matches the CTD mean variations (Fig. 3.19). The largest volume fraction among our data occurred in 1991. However, this was purely TAW, and apart from that year, the highest volume fractions were in 2006, 2012 and 2014, and then combined with rather high fraction of AW. We conclude that summer AW presence has been strong in earlier years, however, never as strong as in 2012–2014, which were all classified as Winter Open years.

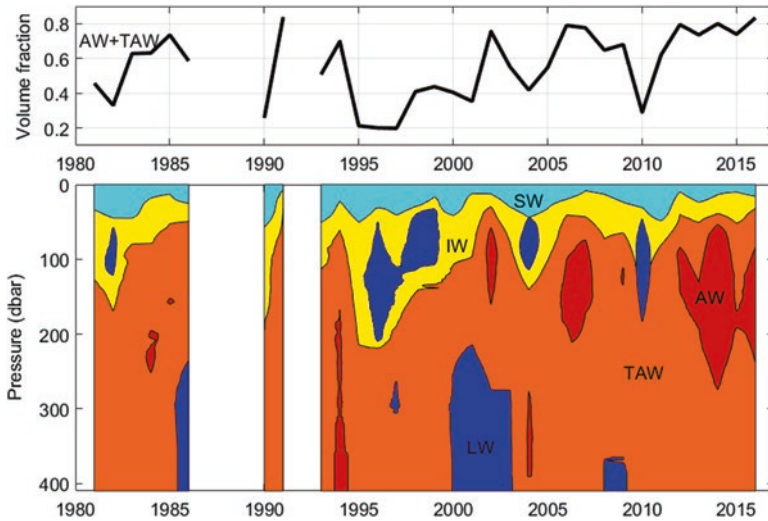


Fig. 3.20 Lower panel: Time series of summer water masses in Kongsfjorden, as defined in Table 3.5, based on the Kongsfjorden transect data. Upper panel: Fraction of total volume of Kongsfjorden that was occupied with Transformed Atlantic Water (TAW) or Atlantic Water (AW). SW Surface Water, IW Intermediate Water, LW Local Water

3.6 Discussion

3.6.1 Seasonal Temperature – Salinity Characteristics

Our main finding from the Kongsfjorden Transect is that inflow of AW during winter is more common than described in the established scenario; that dense water formation inside the fjord prevents AW from entering the fjord basin during the winter season. We have named that established scenario Winter Deep. We call it Winter Intermediate if AW enters the fjord in the deep part of the water column, and Winter Open if the AW inflow includes the surface layer. It appears that the vertical distribution of horizontal density differences across the shelf-edge front determines at which depth the inflowing AW settles on the shelf, and this seems to agree with the behavior of eddy overturning across the front, as argued by Tverberg and Nøst (2009), and illustrated schematically by the sketches of shelf-edge processes (Fig. 3.7). We might see indications that pure topographic steering of AW from the WSC into Kongsfjordrenna, as explained by Nilsen et al. (2016) and illustrated in Fig. 3.7, is most pronounced if density differences across the shelf-edge front are weak. This was the case during winter 2014, leading to the warmest and most saline Kongsfjorden winter water in our database (Fig. 3.12). We also find indications that

whether or not the AW in Kongsfjordrenna enters the fjord, depends on density differences between the fjord and shelf, providing a geostrophic control at the fjord entrance that prevents AW from entering the fjord when fjord water is denser than shelf water. The latter can lead to Winter Deep condition in the fjord. The winter transects of this type (Figs. 3.13 and 3.23) may suggest that Winter Deep is associated with limited AW exchange across the shelf-edge front with AW settling at some intermediate depth in Kongsfjordrenna.

According to our simplified classification, winter inflow of AW at intermediate depth level (Winter Deep) is normally associated with vertical convection to the bottom inside Kongsfjorden. Deep winter inflow of AW (Winter Intermediate) should be associated with vertical convection to intermediate depth, while winter inflow of AW over depths that include the surface (Winter Open) is associated with vertical convection to the bottom of this cooled AW. The only years that do not fit our classifications of winter convection types (Table 3.6) are 1997 and 2009, and possibly 2011, all of them suggested by us to be Winter Deep (see Fig. 3.14), while deep AW inflow is observed (associated with Winter Intermediate). None of these years actually has winter CTD observations from within the fjord basin. However, there are mooring observations from 2009 and 2011. A detailed look at those time series (Fig. 6.2 in Hegseth et al., Chap. 6) reveals that the deep AW advection in 2009 was a single event in April, while before that, deep convection producing LW or WCW was dominating. A somewhat similar development happened in spring 2011, with deep inflow of AW evident in both March and April, but strong convection of LW and WCW prior to that. If the production of WCW has been strong enough, a short period with deep AW advection at the end of the winter may not be sufficient to replace all the deep winter water produced by convection.

The three winter scenarios are followed by summers with distinctly different distributions of water masses in the Kongsfjorden water column (Fig. 3.20). During a summer after a Winter Deep winter, one normally finds remnants of the coldest winter water in the deepest part of the water column, and summer inflow of AW at intermediate depth. After Winter Intermediate winters, remnants of the coldest winter water is normally found at some intermediate depth, and summer inflow of AW below that. The summers after Winter Open winters have similar characteristic water column as summers after Winter Deep winters, except that the winter water is rather warm. One implication of these interannual variations is that, constructing a mean picture from the whole Kongsfjorden Transect data set, will not reflect a realistic seasonal cycle. We refer to the Appendix for a comparison between hydrographic transects from individual years and the overall winter and summer means (Figs. 3.2 and 3.3).

3.6.2 Environmental Forcing

Here we seek to link the changes and variability we see in the water masses in Kongsfjorden to associated environmental changes and variability. So far in the discussion we have focused on how strong and at what depth level is the advection of AW into the fjord. This, we have seen, is closely linked to processes leading to overturning across the shelf-edge front. The strength of eddy overturning can depend on how large is the heat loss to the atmosphere (Tverberg et al. 2014) and on wind conditions (Cottier et al. 2007). Wind conditions at the shelf-edge front governs surface Ekman transport and can affect topographic steering of AW into Kongsfjordrenna (Nilsen et al. 2016). However, the Kongsfjorden Transect data set best illustrates how much the shelf-edge processes depend on the density of the shelf water column, and we propose that this is mainly governed by how much fresh water and drift ice the SPC contains. Earlier, we have looked into how much sea ice forms locally, while the presence of drift ice in the SPC is rather associated with melting of sea ice.

First, we investigate heat loss to the atmosphere, through analysis of surface heat fluxes from reanalysis ERA Interim model data from a position located at the shelf edge; the time series shown in Fig. 3.21. The data are low-pass filtered with a long window of 90 days, so they reveal only the overall seasonal cycle and its deviation from the mean seasonal cycle over 35 years (1980–2014). It appears the winters in the 1990s were relatively cold, while the period from spring 2002 to winter 2009 was warm during both winters and summers. Since 2009, some winters have been cold while others have been warm, and summers have been generally cold. The

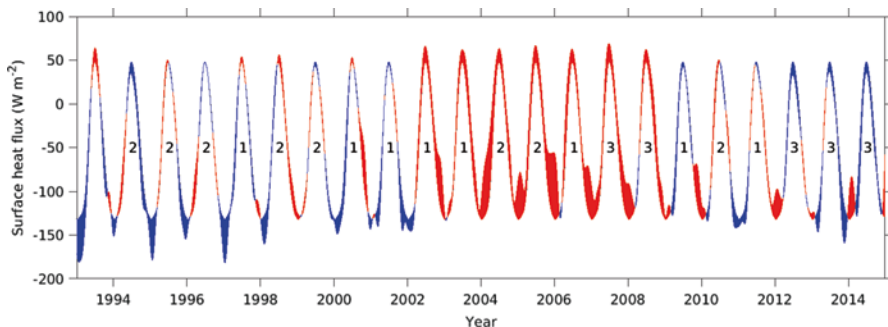


Fig. 3.21 Surface heat flux at position 78°45'N and 009°E, extracted from the European Centre for Medium-Range Weather Forecasts (ECMWF) ERA Interim reanalysis database. The time series has been low-pass filtered with a 90 days window and are shown as deviations from a seasonal mean over 35 years, from 1980 to 2014. Blue indicates negative anomalies ('colder') and red positive anomalies ('warmer'). Numbers indicate winter type associated with each year; 1 indicates "Winter Deep" winters, 2 to "Winter Intermediate" winters and 3 to "Winter Open" winters

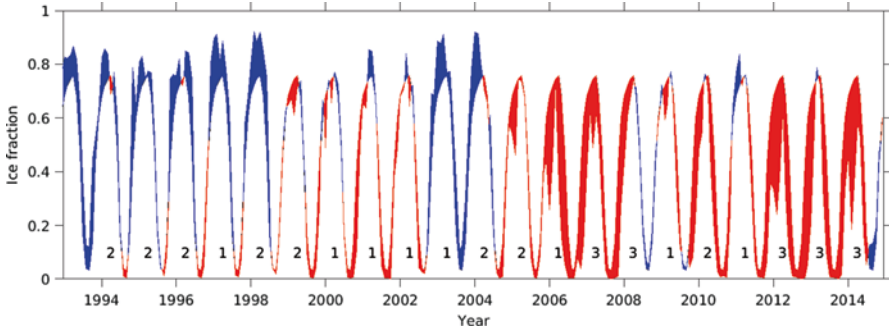


Fig. 3.22 Average sea ice cover fraction in a part of the northern Barents Sea (inside the red rectangle indicated in Fig. 3.1). Data are extracted from monthly means from the National Snow and Ice Data Center (NSIDC) database. The data are shown as deviations from a seasonal mean over 35 years; from 1980 to 2014. Blue indicates positive anomalies (more sea ice) and red negative anomalies (less sea ice). Numbers indicates winter type associated with each year; 1 indicates “Winter Deep” winters, 2 to “Winter Intermediate” winters and 3 to “Winter Open” winters

warm period coincides in time with a period of warm summer AW in the southern part of the WSC (Fig. 3.4). The WSC outside Kongsfjorden is, however, not particularly warm during this period, especially after the Winter Intermediate winters in 2004 and 2005. This can indicate that lateral heat loss (eddies and geostrophic advection) from the WSC is particularly strong during and after Winter Intermediate winters. Other than this, we find no clear effect from varying surface heat flux alone.

We seek information on the potential for drift ice occurring in the SPC on the shelf, by analyzing data on average sea ice cover inside a region of the Barents Sea just east of Svalbard, including Storfjorden (Fig. 3.1). This area is likely to feed drift ice into the coastal current (SPC). We may even suggest that the ice cover there has a direct effect on water mass conditions in the SPC, so a diminishing Arctic ice cap will affect those water mass conditions. The average sea ice cover in this box is shown in Fig. 3.22 as time series of deviations from the mean seasonal cycle, similar to the method applied in Fig. 3.21. Our Kongsfjorden Transect data set indicates that between 1994 and 1999, all winters except for 1997 were Winter Intermediate winters, and they were indeed associated with much sea ice. Even though the Winter Deep winter of 1997 was a winter with much sea ice east of Svalbard, there was an anomalously long period with less sea ice than normal the preceding summer and autumn. After 2000, there have been only two winters with extensive sea ice cover in that region, and one of these winters (2004) was indeed a Winter Intermediate winter. The Winter Open winters are all associated with very low sea ice cover east of Svalbard during the preceding summer and autumn. In such a situation, the SPC will be unusually saline already before the winter, and will easily become denser than the WSC even during relatively warm winters. The Winter Deep winters have mixed ice conditions as well as varying surface heat loss, and some of the Winter

Intermediate winters as well. Summing up our findings, we may suggest that heavy drift ice conditions in the SPC are usually associated with Winter Intermediate winters, while very low sea ice coverage reflects Winter Open winters.

3.6.3 ‘Cold’ and ‘Warm’ Years

Winter Intermediate winters are usually followed by cold summer water masses in the fjord because of remnants of winter convection to intermediate depth (Fig. 3.17). Winter Deep winters on the other hand, can sometimes be followed by warm summers, because of rather shallow and strong AW inflow. The Winter Open winters have generally warm water masses in the fjord, however, they are not consistently followed by particularly warm summers, because the very dense Winter Open winter water can delay summer inflow of AW. The three winter types we have defined are thus not directly linked to ‘warm’ or ‘cold’ years. Hegseth et al. (Chap. 6) refer to the periods 2003–2005 and 2009–2011 as ‘cold’ and the periods 2006–2008 and 2012–2014 as ‘warm’. All these ‘warm’ years we associate with strong AW advection, and all, except 2006, had Winter Open winters. Three of the ‘cold’ years, we have associated with Winter Intermediate winters (2004, 2005, 2010) and two with Winter Deep winters (2003, 2011). These particular Winter Deep winters produced unusually dense winter water (see Fig. 3.14), which may have suppressed AW inflow during the following summer. Year 2009 (Winter Deep) has also been classified as a ‘cold’ year, but only the winter/spring period. Extensive sea ice cover inside Kongsfjorden can be indications of a ‘cold’ year and provide a cold source for the summer water column (due to melting). In fact, the 5 years with most extensive sea ice cover in Kongsfjorden (Fig. 3.10), are all suggested to be ‘cold’ years. The most extensive sea ice cover was observed in March 2004, which, however, had melted by April (Hegseth et al., Chap. 6). Isfjorden had a large fast ice cover in 2004 as well, while there was substantial sea ice production in 2002, 2003 and 2005 (Nilsen et al. 2008). We may assume that somewhat similar conditions apply to Kongsfjorden, although conditions in Isfjorden do not automatically apply to Kongsfjorden. For instance, a study comparing Isfjorden and Kongsfjorden during 2007 (Ledang 2009) showed that Isfjorden was much less influenced by AW advection than Kongsfjorden that year, with Isfjorden containing distinctly fresher water masses. This may be an influence from drift ice in the coastal current, because solely considering the effect of AW advection one would expect the contrary, since Isfjordrenna (Fig. 3.1a) is more easily connected to WSC than any of the other troughs along the West Spitsbergen Shelf (Nilsen et al. 2016). All the ‘warm’ years are associated with least extensive ice cover inside Kongsfjorden (Fig. 3.10). As mentioned before, the warm years are also associated with extremely little sea ice east of Svalbard (except the rather special year 2006), and consequently very little or no drift ice in the coastal current (SPC).

3.6.4 *Tipping Point*

The 2 °C increase in annual mean temperature in Kongsfjorden that suddenly occurred after the massive AW inflow event in February 2006, ‘recovered’ after a few years, followed by three relatively cold years in 2009–2011. However, the period 2012–2016 reveals prevailing large volumes of Atlantic water masses in the fjord during summer, although TS profiles suggest they have followed Winter Deep winters as well as Winter Open winters (Figs. 3.14 and 3.16). Similar inter-annual variations are seen in the Arctic ice cover, explained by climatic feedback mechanisms (Stroeve et al. 2012). Glacier run off during winter appears to mainly affect the inner part of Kongsfjorden; inside the Lovénøyane. The Kongsfjorden Transect data set has indicated to us that the behavior of the AW inflow to Kongsfjorden is very much depending on the density of the shelf water column, thus indirectly being affected by a diminishing Arctic ice cap. Our data suggest that heavy drift ice in the SPC is usually associated with Winter Intermediate winters (Fig. 3.22). We might suggest that the impact of reduced drift ice in the SPC can be, down to a certain threshold, a colder shelf water, either due to increased heat loss to the atmosphere, or somewhat contradictory, more melting by AW from the WSC (in combination leading to Winter Deep winters). In this situation, all the factors we have mentioned in this paper, act together in a delicate balance, making it very hard to relate the strength of one single factor to the density of the shelf water. Only when drift ice extent is below some undetermined threshold, will the temperature and salinity of the shelf water increase due to exchange with AW in the WSC (in combination with heat loss to the atmosphere, leading to very dense shelf water and Winter Open winters). If the Arctic ice cap continues the diminishing trend it has had since 1980 (Xia et al. 2014), the Winter Open winters are likely to become the normal situation in Kongsfjorden, resulting in AW filling the fjord both in winter and summer. In that case, the February 2006 event was a tipping point for the Kongsfjorden environment. A better understanding of the coastal current (SPC) is needed to improve our knowledge of what determines the density of the shelf water column, and should be the focus for future studies. We have not investigated wind effects on shelf-edge processes in this paper, and we feel that the geostrophic control at the fjord entrance is not explained properly as well. Thus, we leave these topics for future studies.

Acknowledgements Ragnheid Skogseth (RS) prepared and shared CTD data from the UNIS Hydrographic database (UNIS HD) with data collected by NPI, UNIS, IOPAN and SAMS or extracted from public databases like The Norwegian Marine Data Centre (NMDC at the imr.no), the PANGAEA database (AWI) and ICES. Funding for RS and the construction of the UNIS HD merits REOCIRC (Remote Sensing of Ocean Circulation and Environmental Mass Changes, a Research Council of Norway project no. 222696/F50). The Norwegian Polar Institute provided CTD data from July 2015 and July 2016 through the MOSJ program. The work contributes as well to the project FjoCon 225218/E40, financed by the Norwegian Research Council. We thank Colin Griffiths for overseeing the SAMS mooring programme supported by the UK Natural Environment Research Council (Oceans 2025 and Northern Sea Program) and the Research Council of Norway (projects Cleopatra: 178766, Cleopatra II: 216537, and Circa: 214271/F20). Contribution by FC and MEI was undertaken through the Scottish Alliance for Geoscience Environment and Society (SAGES).

Appendix A: The Kongsfjorden Transect Hydrography from Individual Years

Here we show temperature, salinity and density distribution for each year with enough available data to construct the Kongsfjorden Transect, separated in Winter Deep, Winter Intermediate and Winter Open winter data (January–May) and their respective following summers (July–September).

The five Winter Deep winters with sufficient CTD data available to grid the transects are shown in Fig. 3.23, although in two of them, 1997 and 2009, the data coverage is poor in the central basin of Kongsfjorden. In 1997, the data coverage is also poor across the shelf-edge front. Focusing on those transects with good data coverage, all these years the WSC had a narrow warm core confined to the shelf-edge region, and reaching the surface. The surface shelf water had similar or lower density than the surface-layer part of the WSC core. The deepest part of the shelf water column was, however, generally denser than the water at the same depth in the WSC core, and the density differences across the front were weak at intermediate depth level.

Such a density distribution favors eddy overturning with AW exchange across the front dominating at the depth level where the density differences vanish, that is intermediate depth (Tverberg and Nøst 2009). This is indeed what can be observed over the shelf. The overturning cell indicated in the principle sketch (Fig. 3.17) of shelf-edge processes, would in such cases apply to the upper part of the water column only. In 2009, AW was found both at intermediate and deep water level, and cross-frontal density differences were weak at both levels. In the transects from the 3 years with good data coverage, it can be seen that Kongsfjorden interior was less influenced by AW than the shelf. We also note that in the mouth region of Kongsfjorden, a depression of the deepest isopycnals is visible each of these years. It may be possible that these depressions are associated with the coastal current at the mouth region of Kongsfjorden forcing the path of AW advection to be modified there (geostrophic control). The exact location of the depressions varies among the years, which may confirm that the location of the geostrophic control is located at the common mouth of Kongsfjorden-Krossfjorden (Kb0) in some years and at the mouth of the Kongsfjorden central basin (Kb1) in others. This is in line with the typical situation during a Winter Deep winter; denser water in the fjord in the deepest part of the water column enhances the bottom speed of the coastal current on the shelf, past the fjord.

Mooring data add valuable information from two of these years; 2006 and 2009. Most of the winter in 2006 was actually a Winter Intermediate winter with exceptionally strong deep AW advection, culminating in a rather short period with strong convection and mixing (see Fig. 3.5), and it must have been during this final part of the winter that the largest volumes of winter water were produced. The winter 2009 was opposite; during most of the winter the mooring data reveal deep convection and only weak indications of AW advection, except from a short period in late April with deep AW inflow (see Fig. 6.2 in Hegseth et al. [this volume](#)). That inflow was evidently not strong enough to replace all the winter water produced earlier that winter.

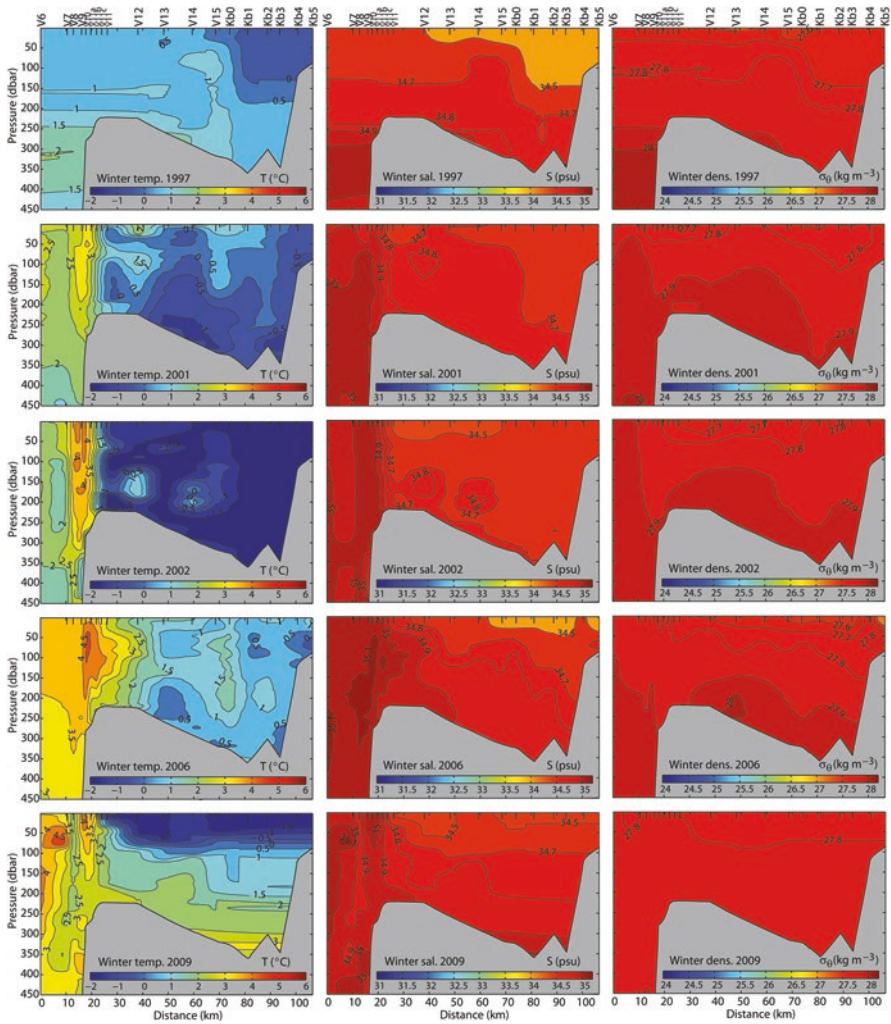


Fig. 3.23 Mean winter temperature, salinity and potential density along the Kongsfjorden transect, based on all available Kongsfjorden Transect data from winters 1997, 2001, 2002, 2006 and 2009, defined as “Winter Deep”

The five Winter Intermediate winters with sufficient CTD data available to grid the transects are shown in Fig. 3.24, although two of them have limited data coverage (1998 and 1999). The data coverage in the WSC, however, is good for all 5 years, revealing a WSC that tends to be isolated from the surface. Shelf water spreads westwards on top of the WSC, and AW from the WSC tends to enter the shelf in the deep water and more pronounced than during the Winter Deep winters. The WSC was clearly denser than shelf water at all depths. This leads to a weakening of the WSC with depth (thermal wind effect), perhaps contributing to enhanced

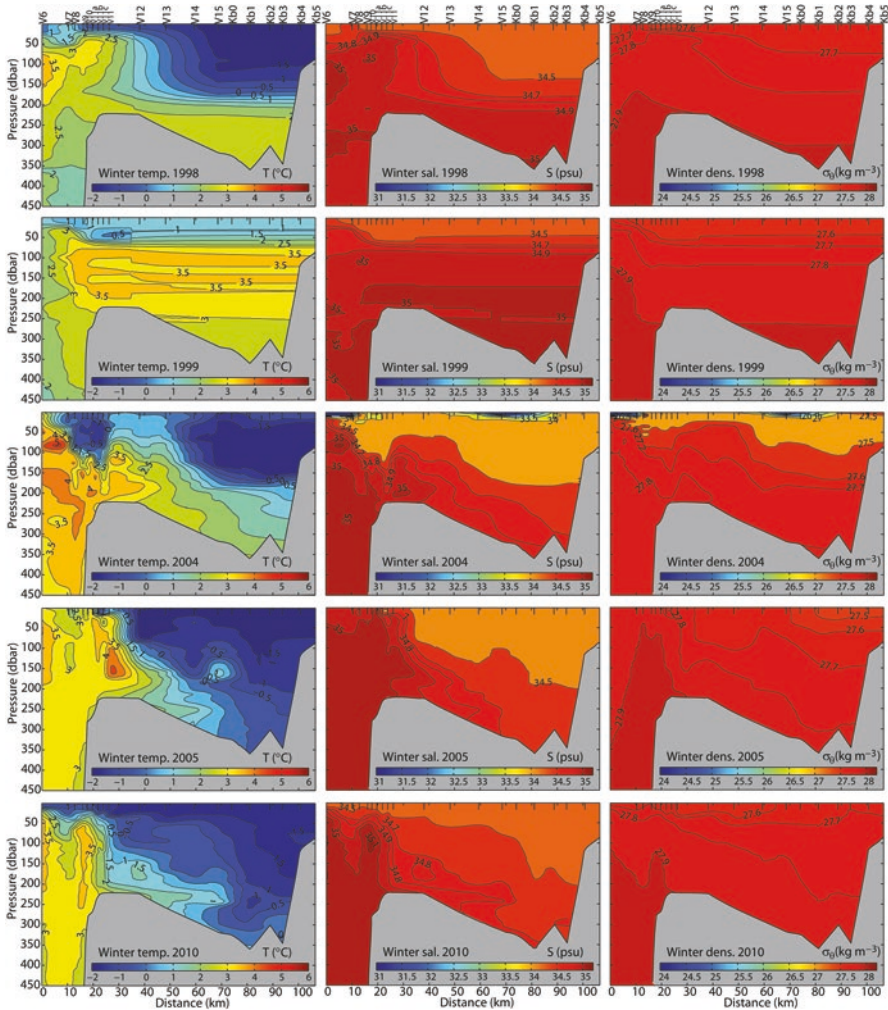


Fig. 3.24 Mean winter temperature, salinity and potential density along the Kongsfjorden transect, based on all available Kongsfjorden Transect data from winters 1998, 1999, 2004, 2005, and 2010, defined as “Winter Intermediate”

baroclinic instabilities at the shelf-edge front. The resulting eddy overturning will bring AW onto the shelf in the deep and shelf water off-shelf in the surface. The water column in Kongsfjorden interior had lower density than the shelf, meaning no geostrophic control at the entrance. Mooring data confirm deep AW advection inside Kongsfjorden during three of these winters (2004, 2005 and 2010), combined with homogeneously cold water above the AW inflow. In 2010, the AW advection reached rather shallow depths in January–March, while it almost disappeared in April–May and was replaced by a thick layer of homogeneously cold water, reaching almost 200 m depth (see Fig. 6.2 in Hegseth et al., Chap. 6).

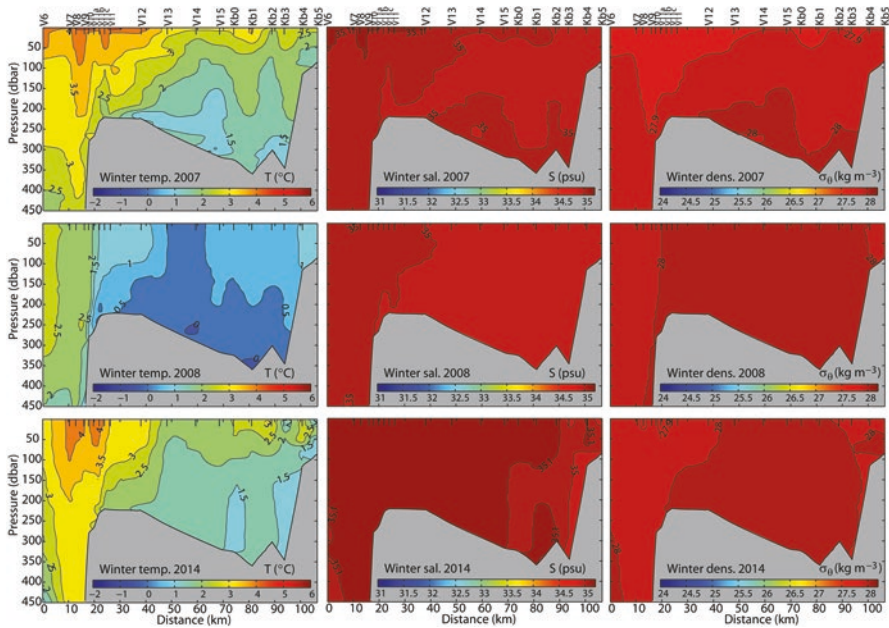


Fig. 3.25 Mean winter temperature, salinity and potential density along the Kongsfjorden transect, based on all available Kongsfjorden Transect data from winters 2007, 2008 and 2014, defined as “Winter Open”

The three Winter Open winters with sufficient CTD data available to make transects (2007, 2008 and 2014) are shown in Fig. 3.25. The WSC reaches the surface, is less dense than shelf water in the whole water column, and tends to spread onto the shelf, being most pronounced in the surface. The thermal wind effect on the WSC in such a situation will enhance the current speed with increasing depth. This might guide the WSC northwards past Kongsfjordrenna at depth, while the eddy overturning will spread AW onto the shelf in the surface layer. However, except for 2007, the density differences were weak, so topographic steering of geostrophic AW advection in Kongsfjordrenna can be significant, with AW advection in the whole water column. In 2007 it looks like the AW might not be passing Kb1 in the deep part of the water column (due to geostrophic control?). In the surface, however, AW entered the fjord freely. The mooring data inside Kongsfjorden indicated a rather homogeneously warm water column, but with a tendency of warmest temperatures in the surface (see Fig. 6.2 in Hegseth et al., Chap. 6). The homogeneously warm water column is particularly evident in the 2012 and 2014 time series, which may indicate no horizontal density differences across the shelf-edge front that year, meaning weak eddy overturning, but substantial geostrophic AW advection, with horizontal eddy diffusion spreading water masses laterally.

The eight summer transects after Winter Deep winters are shown in Fig. 3.26. Inside Kongsfjorden, they are characterized by remnants of cold winter water in the

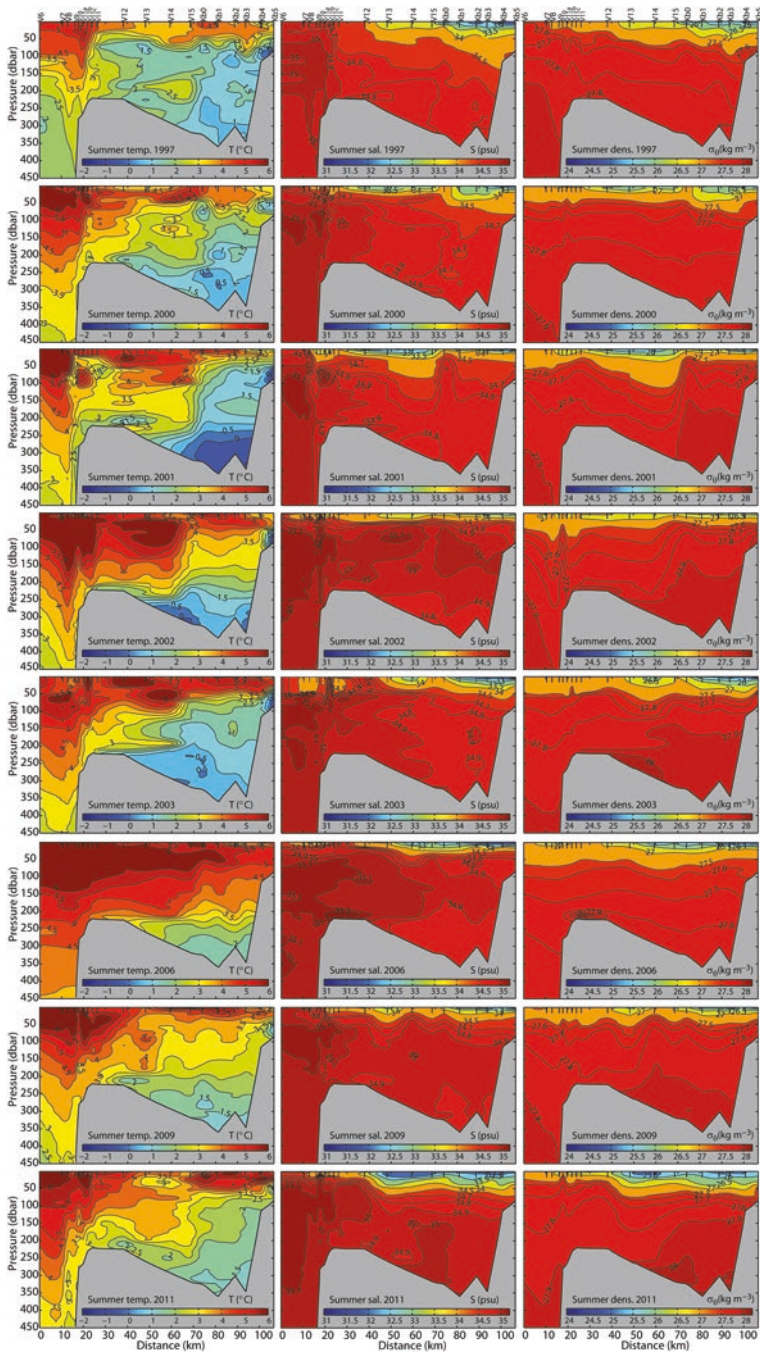


Fig. 3.26 Mean summer temperature, salinity and potential density along the Kongsfjorden Transect data from summers 1997, 2000, 2001, 2002, 2003, 2006, 2009 and 2011, after “Winter Deep” winters

deep, and a core of warm and saline AW or TAW at some intermediate depth. The shelf has in principle the same distribution, however with more pronounced presence of AW or TAW. Some years (e.g., 2001), the deep fjord water was clearly denser than the deep water in Kongsfjordrenna, which indicates that the geostrophic control in the fjord entrance can be in effect throughout long parts of the summer. The AW exchange was extensive across the shelf-edge front, with no pronounced density front. The mooring data confirm rather cold water in the deep in summer 2003 and 2011, while in 2006 and 2009 the cold water resided below the mooring depth (see Fig. 6.2 in Hegseth et al., Chap. 6).

The six summer transects after Winter Intermediate winters are shown in Fig. 3.27 (in 1995 and 1996, the data coverage was too poor to form transects). They are characterized by remnants of cold winter water at intermediate depth level, while AW or TAW were found in the deep. The deep water can comprise remnants of deep AW inflow during the winter, or summer advection of AW. We would expect the summer transects in 2004 and 2010 to be examples of the first situation, because deep fjord water is denser than shelf water, possibly implying geostrophic control at work in the mouth. Mooring data, however, indicate that there was a distinct increase in AW in 2010, similar to 2005 (see Fig. 6.2 in Hegseth et al., Chap. 6), indicating summer advection of AW. Some years the AW exchange across the shelf-edge front appeared to be restricted (e.g. 1998), but in other years it was pronounced (e.g. 2004, 2005, 2010). The shelf-edge front is not a pronounced density front; rather the isopycnals tend to often be terrain following, which can be a long-term effect of eddy exchange across the shelf-edge front (Adcock and Marshall 2000).

The five summer transects after Winter Open winters are shown in Fig. 3.28. They show that large volumes of old winter water were present in the fjord and on the shelf during these summers (winter water from Winter Open winters is relatively warm). The density at intermediate and deep depth levels were generally higher than in the WSC, with two summers (2007 and 2013) being more pronounced in the fjord than on the shelf. Temperature and salinity were generally higher on the shelf than in the fjord. Mooring data confirm a rather warm water column during these summers and only in 2014 there was a pronounced increase in AW content throughout the summer (see Fig. 6.2 in Hegseth et al., Chap. 6). This indicates that there may be rather little water renewal in the fjord during a summer after a Winter Open winter. Our explanation is stronger geostrophic control at the mouth due to the high-density water inside the fjord.

The overall winter mean transects of temperature and salinity (Fig. 3.2) seem dominated by the Winter Deep type of winter, with a water mass close to LW definitions filling most of the shelf and fjord. However, they are strongly influenced by Winter Intermediate and Winter Open winters as well; the shelf-edge front has an overturning leading AW onto the shelf in the deep and shelf water over the WSC (Winter Intermediate), rather high bottom salinity on the shelf and in the fjord (Winter Intermediate), and TAW-type water mass close to Kb3 (Winter Open). Kb3 is the only CTD station in the transect that is placed within the path of the topographic steering of the geostrophic AW advection in the fjord. The influence from the Winter Open (AW) winters will thus likely be strongest there. The overall sum-

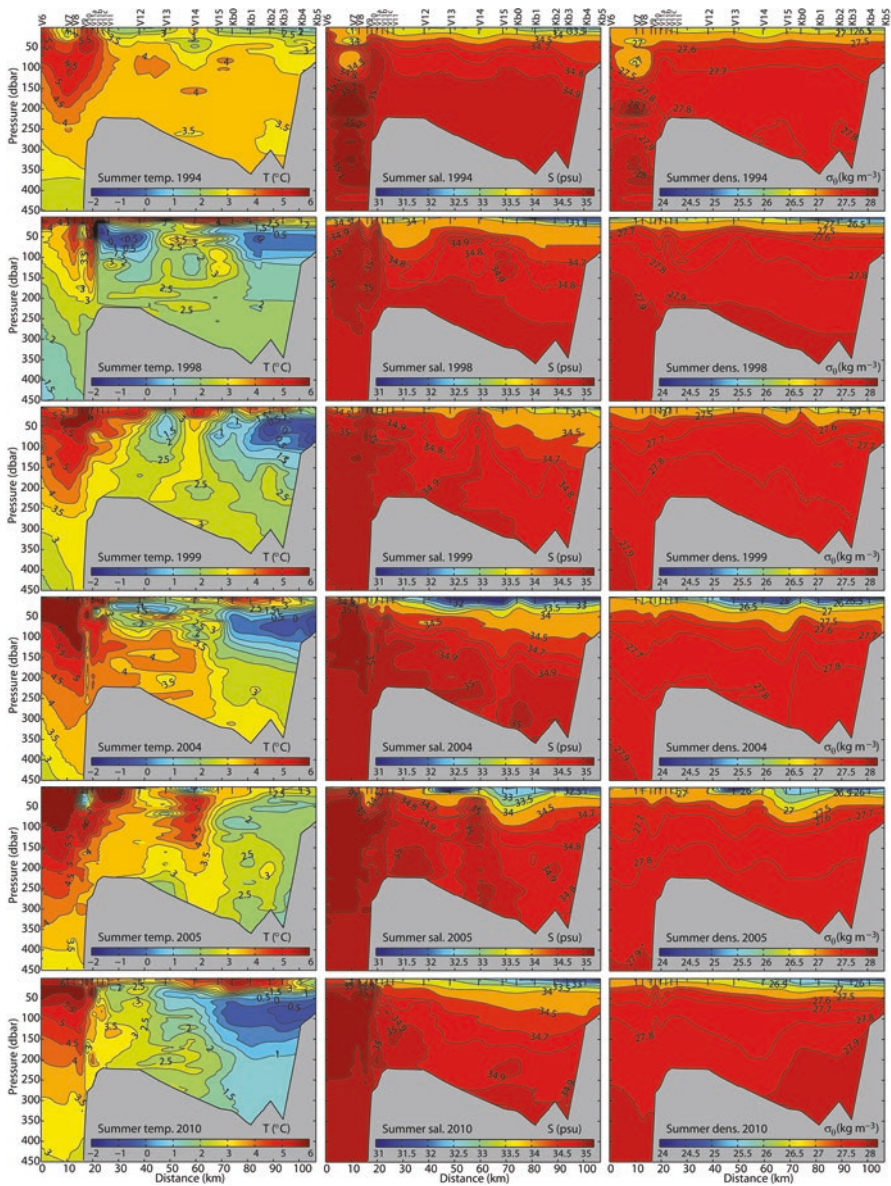


Fig. 3.27 Mean summer temperature, salinity and potential density along the Kongsfjorden transect, based on all available Kongsfjorden Transect data from summers 1994, 1998, 1999, 2004, 2005 and 2010, after “Winter Intermediate” winters

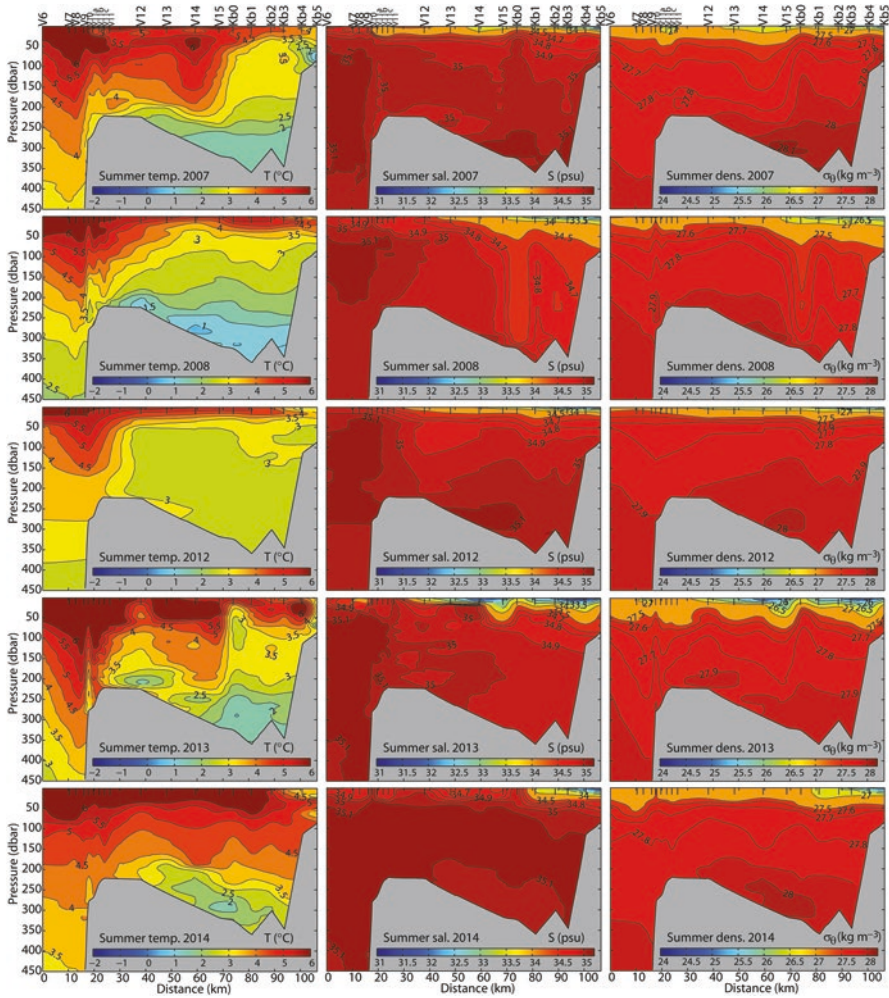


Fig. 3.28 Mean summer temperature, salinity and potential density along the Kongsfjorden transect, based on all available Kongsfjorden Transect data from summers 2007, 2008, 2012, 2013 and 2014, after “Winter Open” winters

mer mean transects of temperature and salinity (Fig. 3.3), display a clear discrepancy between the shelf and fjord regions, which in reality is only seen after some Winter Open winters (Fig. 3.28). The water mass distribution inside the fjord seems like a mixture of summers after a Winter Deep and a Winter Open winter. TAW fills most of the water column below thin layers of SW and IW, and LW is only found at the head of the fjord, reflecting the glacier influence in the basin inside the Lovénøyane (see Table 3.5 for water mass definitions). A summer after a Winter Deep winter would have had LW in the deepest part of the water column, while a summer after a Winter Open winter would have pure AW instead of TAW filling part

of the water column. Comparing these mean summer sections with the time series of water mass distribution in Kongsfjorden (Fig. 3.20), we see that such a distribution has been the most common after 2006, more specifically the two periods 2006–2008 and 2012–2014.

- Data Availability: doi:10.21334/npolar.2019.074a215c.

References

- Adcock ST, Marshall DP (2000) Interactions between geostrophic eddies and the mean circulation over large-scale bottom topography. *J Phys Oceanogr* 30:3223–3238
- Boyd TJ, D'Asaro EA (1994) Cooling of the West Spitsbergen current: wintertime observations west of Svalbard. *J Geophys Res* 99:22597–22618
- Cokelet ED, Tervalon N, Bellingham JG (2008) Hydrography of the West Spitsbergen current, Svalbard Branch: Autumn 2001. *J Geophys Res* 113. <https://doi.org/10.1029/2007JC004150>
- Collings IL, Grimshaw R (1980) The effect of topography on the stability of a barotropic coastal current. *Dyn Atmos Oceans* 10:83–106
- Cottier F, Tverberg V, Svendsen H, Griffiths C, Inall M (2003) Water mass modification and exchange in an arctic fjord (poster). In: EGS-AGU-EUG Joint assembly, Nice, France
- Cottier F, Tverberg V, Inall M, Svendsen H, Nilsen F, Griffiths C (2005) Water mass modification in an Arctic fjord through cross-shelf exchange: the seasonal hydrography of Kongsfjorden, Svalbard. *J Geophys Res* 110. <https://doi.org/10.1029/2004JC002757>
- Cottier FR, Nilsen F, Inall ME, Gerland S, Tverberg V, Svendsen H (2007) Wintertime warming of an Arctic shelf in response to large-scale atmospheric circulation. *Geophys Res Lett* 34. <https://doi.org/10.1029/2007GL029948>
- Cottier F, Nilsen F, Skogseth R, Tverberg V, Skarðhamar J, Svendsen H (2010) Arctic fjords: a review of the oceanographic environment and dominant physical processes. In: *Fjord systems and archives*, Geological society special publication 344. Geological Society, London, pp 35–50
- Emery WJ, Thomson RE (2014) *Data analysis methods in physical oceanography*, 3rd edn. Elsevier Science, Amsterdam, 728 pp. isbn:978-0-123-87782-6
- Furevik T (2001) Annual and interannual variability of Atlantic Water temperatures in the Norwegian and Barents Seas: 1980–1996. *Deep-Sea Res I Oceanogr Res Pap* 48:383–404. [https://doi.org/10.1016/S0967-0637\(00\)00050-9](https://doi.org/10.1016/S0967-0637(00)00050-9)
- Gerland S, Renner AHH (2007) Sea-ice mass-balance monitoring in an Arctic fjord. *Ann Glaciol* 46:435–442
- Gjevik B, Straume T (1989) Model simulations of the M2 and the K1 tide in the Nordic Seas and the Arctic Ocean. *Tellus* 41A:73–96
- Hegseth EN, Assmy P, Wiktor J, Kristiansen S, Leu E, Piquet AMT, Tverberg V, Cottier F (this volume-b) Chapter 6: Phytoplankton seasonal dynamics in Kongsfjorden, Svalbard and the adjacent shelf. In: Hop H, Wiencke C (eds) *The ecosystem of Kongsfjorden, Svalbard*, *Advances in polar ecology* 2. Springer, Cham
- Helland-Hansen B, Nansen F (1909) *The Norwegian Sea. Its physical oceanography based upon the Norwegian researches 1900–1904. vol 2. Report on Norwegian Fishery and Marine-Investigations*. Det Mallinske Bogtrykkeri, Kristiania
- Hop H, Pearson T, Hegseth EN, Kovacs KM, Wiencke C, Kwasniewski S, Eiane K, Mehlum F, Gulliksen B, Włodarska-Kowalczyk M, Lydersen C, Weslawski JM, Cochrane S, Gabrielsen GW, Leakey RJG, Lønne OJ, Zajaczkowski M, Falk-Petersen S, Kendall M, Wängberg S-Å, Bischof K, Voronkov AY, Kovaltchouk NA, Wiktor J, Poltermann M, di Prisco G, Papucci C, Gerland S (2002) The marine ecosystem of Kongsfjorden, Svalbard. *Polar Res* 21:167–208

- Hopkins TS (1991) The GIN Sea – a synthesis of its physical oceanography and literature review 1972–1985. *Earth Sci Rev* 30:175–318
- Inall ME, Nilsen F, Cottier FR, Daae R (2015) Shelf/fjord exchange driven by coastal-trapped waves in the Arctic. *J Geophys Res* 120:8283–8303
- Ingvaldsen R, Bø-Reitan M, Svendsen H, Asplin L (2001) The upper layer circulation in Kongsfjorden and Krossfjorden – a complex fjord system on the west coast of Spitsbergen. *Mem Natl Inst Polar Res Spec Issue* 54:393–407
- Kimura S, Holland PR, Jenkins A, Piggott M (2014) The effect of meltwater plumes on the melting of a vertical glacier face. *J Phys Oceanogr* 44:3099–3117. <https://doi.org/10.1175/JPO-D-13-0219.1>
- Klinck JM, O'Brien J, Svendsen H (1981) A simple model of fjord and coastal circulation interaction. *J Phys Oceanogr* 11:1612–1626
- Ledang AB (2009) Coupled physical and biological processes related to mesoscale eddy field in Kongsfjorden and Isfjorden. Master thesis. University of Bergen, Bergen, 89 pp
- Loeng H (1991) Features of the physical oceanographic conditions of the Barents Sea. *Polar Res* 10:5–18
- Luckman A, Benn DI, Cottier F, Bevan S, Nilsen F, Inall M (2015) Calving rates at tidewater glaciers vary strongly with ocean temperature. *Nat Commun* 6:1–7. <https://doi.org/10.1038/ncomms9566>
- Lydersen C, Assmy P, Falk-Petersen S, Kohler J, Kovacs KM, Reigstad M, Steen H, Strøm H, Sundfjord A, Varpe Ø, Walczowski W, Weslawski JM, Zajaczkowski M (2014) The importance of tidewater glaciers for marine mammals and seabirds in Svalbard, Norway. *J Mar Syst* 129:452–471
- MacLachlan SE, Cottier FR, Austin WEN, Howe JA (2007) The salinity:δ O water relationship in Kongsfjorden, western Spitsbergen. *Polar Res* 26:160–167
- Marshall J, Radko T (2003) Residual-mean solutions for the Antarctic Circumpolar Current and its associated overturning circulation. *J Phys Oceanogr* 33:2341–2354
- Marshall J, Shuckburgh E, Jones H, Hill C (2006) Estimates and implications of surface eddy diffusivity in the southern ocean derived from tracer transport. *J Phys Oceanogr* 36:1806–1821
- McDougall TJ, Barker PM (2011) Getting started with TEOS-10 and the Gibbs Seawater (GSW) Oceanographic Toolbox, 28 pp., SCOR/IAPSO WG127, ISBN 978-0-646-55621-5
- Millero FJ, Feistel R, Wright DG, McDougall TJ (2008) The composition of Standard Seawater and the definition of the Reference-Composition Salinity Scale. *Deep-Sea Res I Oceanogr Res Pap* 55:50–72. <https://doi.org/10.1016/j.dsr.2007.10.001>
- Moffat C (2014) Wind-driven modulation of warm water supply to a proglacial fjord, Jorge Montt Glacier, Patagonia. *Geophys Res Lett* 41:3943–3950. <https://doi.org/10.1002/2014GL060071>
- Mysak LA, Schott F (1977) Evidence for baroclinic instability of the Norwegian Current. *J Geophys Res* 82:2087–2095
- Nilsen F, Gjevik B, Schauer U (2006) Cooling of the West Spitsbergen Current: Isopycnal diffusion by topographic vorticity waves. *J Geophys Res* 111:1–16. <https://doi.org/10.1029/2005JC002991>
- Nilsen F, Cottier F, Skogseth R, Mattsson S (2008) Fjord-shelf exchanges controlled by ice and brine production: the interannual variation of Atlantic Water in Isfjorden, Svalbard. *Cont Shelf Res* 28:1838–1853
- Nilsen F, Skogseth R, Vaardal-Lunde J, Inall M (2016) A simple shelf circulation model: intrusion of Atlantic Water on the West Spitsbergen Shelf. *J Phys Oceanogr* 46:1209–1230. <https://doi.org/10.1175/JPO-D-15-0058.1>
- Notz D, Worster MG (2008) In situ measurements of the evolution of young sea ice. *J Geophys Res* 113:1–7. <https://doi.org/10.1029/2007JC004333>
- Onarheim I, Smedsrud LH, Ingvaldsen R, Nilsen F (2014) Loss of sea ice during winter north of Svalbard. *Tellus A* 66:1–9
- Pavlova O, Gerland S, Hop H (this volume-b) Chapter 4: Changes in sea-ice extent and thickness in Kongsfjorden, Svalbard, and related ecological implications. In: Hop H, Wiencke C (eds) *The ecosystem of Kongsfjorden, Svalbard, Advances in polar ecology* 2. Springer, Cham

- Polyakov IV, Beszczynska A, Carmack EC, Dmitrenko IA, Fahrbach E, Frolov IE, Gerdes R, Hansen E, Holfort J, Ivanov VV, Johnson MA, Karcher M, Kauker F, Morison J, Orvik KA, Schauer U, Simmons HL, Skagseth Ø, Sokolov VT, Steele M, Timokhov LA, Walsh JE (2005) One more step towards a warmer Arctic. *Geophys Res Lett* 32:1–4. <https://doi.org/10.1029/2005GL023740>
- Rudels B, Anderson LG, Jones EP (1996) Formation and evolution of the surface mixed layer and halocline of the Arctic ocean. *J Geophys Res* 101:8807–8821
- Rudels B, Meyer R, Fahrbach E, Ivanov VV, Østerhus S, Quadfasel D, Schauer U, Tverberg V, Woodgate R (2000) Water mass distribution in Fram Strait and over the Yermak Plateau in summer 1997. *Ann Geophys* 18:687–705
- Salcedo-Castro J, Bourgault D, Bentley SJ, deYoung B (2013) Non-hydrostatic modeling of cohesive sediment transport associated with a subglacial buoyant jet in glacial fjords: a process-oriented approach. *Ocean Mod* 63:30–39. <https://doi.org/10.1016/j.ocemod.2012.12.005>
- Saloranta TM, Haugan PM (2004) Northward cooling and freshening of the warm core of the West Spitsbergen Current. *Polar Res* 23:79–88
- Saloranta TM, Svendsen H (2001) Across the Arctic front west of Spitsbergen: high-resolution CTD sections from 1998–2000. *Polar Res* 20:177–184
- Skarðhamar J, Svendsen H (2010) Short-term hydrographic variability in a stratified Arctic fjord. In: *Fjord systems and archives*, Geological society special publication 344. Geological Society, London, pp 51–60
- Steele M, Morison J, Curtin TB (1995) Halocline water formation in the Barents Sea. *J Geophys Res* 100:881–894
- Stroeve JC, Serreze MC, Holland MM, Kay JE, Malanik J, Barrett AP (2012) The Arctic's rapidly shrinking sea ice cover: a research synthesis. *Clim Chang* 110:1005–1027. <https://doi.org/10.1007/s10584-011-0101-1>
- Sundfjord A, Albretsen J, Kasajima Y, Skogseth R, Kohler J, Nuth C, Skarðhamar J, Cottier F, Nilsen F, Asplin L, Gerland S, Torsvik T (2017a) Effects of glacier runoff and wind on surface layer dynamics and Atlantic water exchange in Kongsfjorden, Svalbard: a model study. *Estuar Coast Shelf Sci* 187:260–272. <https://doi.org/10.1016/j.ecss.2017.01.015>
- Svendsen H, Beszczynska-Möller A, Hagen JO, Lefauconnier B, Tverberg V, Gerland S, Ørbæk JB, Bischof K, Papucci C, Zajaczkowski M, Azzolini R, Bruland O, Wiencke C, Winther J-G, Dallmann W (2002) The physical environment of Kongsfjorden-Krossfjorden, and Arctic fjord system in Svalbard. *Polar Res* 21:133–166
- Swift JH (1986) The Arctic waters. In: *The Nordic seas*. Springer, New York, pp 124–153
- Teigen SH, Nilsen F, Gjevik B (2010) Barotropic instability in the West Spitsbergen Current. *J Geophys Res* 115:1–18. <https://doi.org/10.1029/2009JC005996>
- Teigen SH, Nilsen F, Skogseth R, Gjevik B, Beszczynska-Möller A (2011) Baroclinic instability in the West Spitsbergen current. *J Geophys Res* 116:1–20. <https://doi.org/10.1029/2011JC006974>
- Tverberg V, Nøst OA (2009) Eddy overturning across a shelf edge front: Kongsfjorden, west Spitsbergen. *J Geophys Res* 114:1–15. <https://doi.org/10.1029/2008JC005106>
- Tverberg V, Nilsen F, Goszczko I, Cottier F, Svendsen H, Gerland S (2008) The warm winter temperatures of 2006 and 2007 in the Kongsfjorden water masses compared to historical data. In: *Proceedings 8th Ny-Ålesund seminar*, Cambridge. Polarnet Technical Report – 1/2008, pp 40–43
- Tverberg V, Nøst OA, Lydersen C, Kovacs KM (2014) Winter Sea ice melting in the Atlantic water subduction area, Svalbard Norway. *J Geophys Res* 119:5945–5967. <https://doi.org/10.1002/2014JC010013>
- Urbanski JA, Stempniewicz L, Węslawski JM, Dragańska-Deja K, Wochna A, Goc M, Iliszko L (2017) Subglacial discharges create fluctuating foraging hotspots for sea birds in tidewater glacier bays. *Sci Rep* 7:43999. <https://doi.org/10.1038/srep43999>
- Walczowski W (2014) Atlantic water in the Nordic seas. Properties, variability, climatic importance. *GeoPlanet: Earth Planet Sci*, 174 pp. <https://doi.org/10.1007/978-3-319-01279-7>
- Walczowski W, Piechura J (2007) Pathways of the Greenland Sea warming. *Geophys Res Lett* 34:1–5. <https://doi.org/10.1029/2007GL029974>

- Wallace MI, Cottier FR, Berge J, Tarling GA, Griffiths C, Brierley AS (2010) Comparison of zooplankton vertical migration in an ice-free and a seasonally ice-covered Arctic fjord: an insight into the influence of sea ice cover on zooplankton behavior. *Limnol Oceanogr* 55:831–845
- Weslawski JM, Adamski P (1987) Warm and cold years in south Spitsbergen coastal marine ecosystem. *Pol Polar Res* 8:95–106
- Xia W, Xie H, Ke C (2014) Assessing trend and variation of Arctic sea-ice extent during 1979–2012 from latitude perspective of ice edge. *Polar Res* 33:1–13. <https://doi.org/10.3402/polar.v33.21249>